

Development of Products and Procedures for the Mitigation of Tsunami Hazards at Maritime Facilities in Northland



eCoast Limited
Marine Consulting and Research
P.O. Box 151
Raglan, New Zealand

jose@ecoast.co.nz

<BLANK PAGE>

Development of Products and Procedures for the Mitigation of Tsunami Hazards at Maritime Facilities in Northland

Report Status

Version	Date	Status	Approved By:
V2	30 June 2019	Final Report	JCB
V3	5 July 2019	Final Report	SMO

Jose C. Borrero Ph.D.
Sam O'Neill M.Sc.



Cover Picture: Marsden Point at the entrance to Whangarei Harbour, Northland.

The information, including the intellectual property, contained in this report is confidential and proprietary to eCoast Limited. It may be used by the persons to whom it is provided for the stated purpose for which it is provided and must not be imparted to any third person without the prior written approval of eCoast. eCoast Limited reserves all legal rights and remedies in relation to any infringement of its rights in respect of its confidential information.

<BLANK PAGE>

EXECUTIVE SUMMARY

This report describes the development of planning and response products for the mitigation of tsunami hazards from distant and regional source tsunamis affecting maritime facilities in the Northland region. The products are a series of hazard maps and decision-making worksheets (i.e. 'playbooks') designed for use by local emergency management officials and harbourmasters during a tsunami event to guide their response activities as the event unfolds.

The Northland region is ideal for this type of project as it has a high tsunami hazard, a relatively long and well documented tsunami history and a wide variety of maritime assets including a large commercial port, multiple small boat harbours, ferry services and a cruise ship terminal. Additionally, Tutukaka Harbour in Northland is a well-known tsunami 'hot spot' that amplifies incident tsunami energy causing strong and damaging tsunami currents.

The products are based on detailed hydrodynamic modelling of tsunami heights and currents for 72 individual tsunami source locations around the Pacific Rim. Each tsunami source is modelled at three magnitudes, M_w 8.7, 9.0 and 9.3. Detailed modelling was conducted for seven sites in the Northland Region including Doves Bay, Marsden Point, Opuia, Tutukaka, Waitangi, the entrance to Whangaroa Harbour and the inner portion of Whangaroa Harbour.

The outputs from this project are designed for use by Civil Defence and Emergency Management personnel and maritime officers of the Northland Regional Council enabling them to respond appropriately and in a timely manner to a particular tsunami event. The hazard maps include predicted tsunami heights, current speeds and estimates of the duration of the hazardous tsunami currents for a wide range of potential tsunami events. It is hoped that the results of this study will serve as a template or blueprint for the development of port and marina-specific tsunami response plans throughout New Zealand.

CONTENTS

EXECUTIVE SUMMARY	I
TABLE OF FIGURES	III
TABLE OF TABLES.....	V
1 INTRODUCTION	6
1.1 PREVIOUS STUDIES ON TSUNAMI HAZARDS IN NORTHLAND.....	6
1.1.1 <i>The NIWA Studies (2006-2010)</i>	6
1.1.2 <i>Other Reports and Studies</i>	8
1.2 DEVELOPMENT OF MARITIME TSUNAMI PLANNING TOOLS AND PRODUCTS	10
1.3 STUDY SITES	11
2 HISTORY OF TSUNAMIS AFFECTING NORTHLAND	12
2.1 PREHISTORIC TSUNAMI RECORDS.....	12
2.2 HISTORIC TSUNAMI RECORDS	13
3 MODELLING APPROACH	16
3.1 USING COMMIT TO MODEL TSUNAMI CURRENTS	17
3.2 A NOTE ON TERMINOLOGY	20
3.3 NUMERICAL MODELLING GRIDS	21
3.4 TSUNAMI SOURCES	23
3.5 TSUNAMI TRAVEL TIMES	24
4 VALIDATION OF THE COMMIT MODEL TSUNAMIS AFEECTING NORTHLAND. .	26
4.1 CASE 1: THE FEBRUARY 27, 2010 MAULE, CHILE EARTHQUAKE AND TSUNAMI	26
4.2 CASE 2: THE MARCH 11, 2011 TOHOKU EARTHQUAKE AND TSUNAMI.....	27
4.3 CASE 3: THE SEPTEMBER 2 ND , 2016 EAST CAPE EARTHQUAKE AND TSUNAMI.....	28
4.4 MODELLING THE 1976 EVENT IN TUTUKAKA	32
4.4.1 <i>1976 Source Sensitivity Assessment</i>	35
5 FAR-FIELD SENSITIVITY ANALYSIS	38
6 DEVELOPMENT OF MARITIME GUIDANCE PLAYBOOKS	43
6.1 INDIVIDUAL PRODUCTS DERIVED FROM MODEL OUTPUT	43
6.2 SAMPLE PLAYBOOK PAGES	47
6.3 PLAYBOOKS FOR HISTORICAL EVENT SCENARIOS	50
7 CONCLUSIONS	51
8 REFERENCES	52

TABLE OF FIGURES

Figure 1.1 Tsunami hazard and risk levels for Northland proposed by Chagué-Goff <i>et al.</i> , 2006.....	7
Figure 1.2 Modelled tsunami current speeds at Tutukaka for a large magnitude tsunami from South America representative of the 1868 Arica event. (top) NIWA modelling results. (bottom) results from this study. Note: 1 knot = ~2 m/s.....	9
Figure 1.3 Location map for study sites and other locations mentioned in the text.	11
Figure 2.1 Locations of prehistoric tsunami deposits or evidence in Northland.	12
Figure 2.2 The locations of evidence related to three separate prehistoric tsunami events believed to have affected Northland (from Goff <i>et al.</i> , 2010a).....	13
Figure 3.1 The ComMIT propagation model database for tsunamis in the world’s oceans. Insets show the details of the source zone discretization into rectangular sub-faults. .	16
Figure 3.2 Validation and comparison of numerical simulation tools for water surface elevation and currents in Crescent City, CA; (a) comparison of MOST (blue solid), Boussinesq (green dashed), and tide station data (red solid + dots) for the 2011 Tohoku tsunami; (b) comparison of MOST (blue solid) and tide station data (red solid + dots) for 60 h post-EQ; (c) comparison of fluid speed (m/s) at inner boat basin entrance between Boussinesq (yellow) and digitized video data (red solid + dots); (d) comparison of fluid speed (m/s) at inner boat basin entrance between MOST (yellow) and digitized video data (red solid + dots); (e) maximum speed predicted by COULWAVE across a range of different tsunami sources; and (f) maximum speed predicted by MOST across a range of different tsunami sources. (reproduced from Lynett <i>et al.</i> , 2014).	18
Figure 3.3 Modelled maximum tsunami current speeds at the Port of Salalah during the 2004 Indian Ocean tsunami. Black trace represents the estimated path of the Maersk Mandraki container ship as it drifted through port after it was torn from its mooring by the tsunami currents (see Okal <i>et al.</i> , 2006b). Figure reproduced from Borrero, 2017.	19
Figure 3.4 Modelled vs. measured tsunami heights (top) and current speeds (bottom) from the 2011 Japan tsunami at the entrance to Tauranga Harbour using the MOST/ComMIT model. Figure reproduced from Borrero <i>et al.</i> , 2015.	19
Figure 3.5 Definition sketch for tsunami height, flow depth, runup and inundation distance.	20
Figure 3.6 Extents of the A level (green) and B level (red) grids.....	22
Figure 3.7 Extents of the B level (red) and C level (yellow) grids.....	22
Figure 3.8 Tsunami source regions for the tsunami modelling.....	24
Figure 3.9 Tsunami travel times to Northland (red star). The 72 source locations are shown with black dots while the tsunami travel times are shown as white contours.	25
Figure 4.1 Tsunami source model (left) and the trans-pacific propagation pattern (right) for the 2010 Maule, Chile tsunami. Slip amounts (in meters) for the individual fault segments are indicated in white.	26
Figure 4.2 Modelled water level time series compared to measured data at the Marsden Point tide gauge for the 2010 Maule, Chile tsunami.	26

Figure 4.3 Tsunami source model (left) and the trans-pacific propagation pattern (right) for the 2011 Tohoku, Japan tsunami. Slip amounts (in meters) for the individual fault segments are indicated in white.....27

Figure 4.4 Modelled water level time series compared to measured data at Marsden Point for the 2011 Tohoku, Japan tsunami.27

Figure 4.5 Source location of the September 2nd East Cape Earthquake (USGS, 2017)...29

Figure 4.6 (following page) Top panel: Earthquake source model for the September 2nd, 2016 East Cape earthquake (reproduced from USGS, 2016). The top panel shows the location of the fault plane (white region). Epicentre of the mains shock is indicated by a star with aftershocks indicated by black circles. Coloured patches indicate coseismic slip amounts according to the colour scale. The thin red line is the top of the fault plane. The white line is the axis of the Tonga-Kermadec Trench. The purple rectangle shows the location of a 100x50 km fault plane source available in the ComMIT tsunami modelling database. Bottom panel: A detail of the slip distribution along the fault plane with the amount of slip indicated by the colour scale. The location of the earthquake hypocentre is indicated by the star with the arrows indicating the direction of the rupture displacement. The contour lines are the timing (in seconds) of the rupture. The red arrow at the top of the fault plane corresponds to the red arrow in the upper panel. The purple box shows the dimensions of a 100x50 km fault plane.....29

Figure 4.7 Modelled (blue and black traces) versus measured (red trace) water levels at Lottin Point (top) and Tauranga (bottom) for the 2nd September 2016 tsunami.31

Figure 4.8 Photos from a newspaper account of the 1976 tsunami in Tutukaka. The caption reads “[Left]: A yacht heads out to sea at Tutukaka to escape the tidal wave. In the foreground men steady a pile loosened by surging water. [Right]: Mr D. Cutfield, owner of the launch Willie O inspects a pile snapped off at the base.32

Figure 4.9 The source segments (left) and the trans-Pacific propagation pattern.....33

Figure 4.10 Time series of modelled tsunami water level inside Tutukaka Harbour.33

Figure 4.11 Modelled Maximum tsunami amplitude (top) and current speed (bottom).34

Figure 4.12 Source segments and slip amounts for the January 1976 Kermadec earthquake and tsunami.36

Figure 4.13 Comparison of modelled time series outputs at Tutukaka for the 13 different source scenarios. The black line is Source 5, the one used in the initial modelling shown in Figure 4.9 through Figure 4.11.....37

Figure 5.1 Tsunami source regions. Black dots denote the centre of each individual tsunami source.....39

Figure 5.2 Maximum height by source around northern New Zealand.40

Figure 5.3 Maximum height by source for the Bay of Islands area.41

Figure 5.4 (next page) Maximum height by source (left column) and maximum current speed by source (right column) for Tutukaka.....41

Figure 6.1 Trans-Pacific propagation. Tsunami height in cm.....44

Figure 6.2 Maximum tsunami amplitudes in the regional and high-resolution local grids (Tutukaka, Source 10, Magnitude 9.0).....44

Figure 6.3 Time series at 2 locations in C grid, height expressed in cm.45

Figure 6.4 Maximum tsunami induced currents (knots) in discrete colour palette.....	45
Figure 6.5 Tsunami current speed duration over threshold plot.....	46
Figure 6.6 Tsunami current speed vs. depth scatter plot.	46
Figure 6.7 Sample of the navigation flow through the playbook pages.....	48
Figure 6.8 Worksheet pages that should be printed and written on during an event response.	49
Figure 6.9 Sample playbook sheet for the AD 1700 Cascadia Subduction Zone tsunami affecting Tutukaka.	50

TABLE OF TABLES

Table 2.1 Summary of some historical tsunami events and effects in Northland.....	14
Table 3.1 The details of the various computational grids.....	21
Table 3.2 Slip amounts (in meters) applied to each segment in the sensitivity study.	23
Table 5.1 Source numbers contributing to the maximum tsunami amplitudes observed at each region.....	39

1 INTRODUCTION

The objective of this study is to quantify the tsunami hazard at maritime facilities in the Northland region and produce a set of decision-making tools for use by emergency management and the operators of maritime facilities during tsunami events.

1.1 *Previous Studies on Tsunami Hazards in Northland*

There have been numerous reports prepared that focus on tsunami effects in Northland. However, these reports have focussed primarily on overland tsunami inundation resulting from very large or 'maximum credible event' (MCE) type sources.

Written in 2004, the Beetham (2004) report gives a broad-brush overview of tsunami hazards in Northland. Possibly because this report was written in the era before the 2004 Sumatra-Andaman tsunami and the 2011 Tohoku Japan tsunami, the report fails to identify the Tonga-Kermadec (TK) Trench as an important potential tsunami source. Instead the authors focus on potential volcanic sources associated with the TK Trench as the largest near-source hazard. Indeed, the authors state:

“The locally most damaging tsunamis for the Northland region are likely to be generated by volcanic eruptions along the Tonga-Kermadec Trench – at for example the recently discovered Healy Caldera, only 275 km from Northland. There have been no large eruptions in this area in the last 160 years.”

This is an odd conclusion given the fact that a damaging tectonically generated tsunami from the TK Trench affected Northland in 1976.

1.1.1 **The NIWA Studies (2006-2010)**

From 2006 through 2010 a series of five tsunami hazard studies were commissioned by the Northland Regional Council and conducted by NIWA. The first study in this series (Chagué-Goff and Goff, 2006) undertook a comprehensive literature review of tsunami hazards for Northland. This included a review of palaeotsunami evidence, historical information as well as contemporaneous archaeological studies and a sediment stratigraphy analysis for the identification of palaeotsunami deposits.

The study noted that four moderate tsunamis (heights of 1-5 m) had affected the Northland region in the past 150 years while palaeotsunami evidence suggested that at least one large event had occurred in the preceding 600 years. They identified the South American Subduction Zone as a frequent source of moderate to large distant source tsunami. They noted that other source regions such as Indonesia and the Southwest Pacific (Solomon Islands, New Hebrides) are poorly represented in the historical record if at all. They also noted that while a large regional event (such as from the TK Trench) had not occurred in historical times, there was evidence to suggest such an event had occurred in the past 600 years. Ultimately, they proposed that a moderate hazard and risk level be assigned to Northland's east coast with a high hazard and moderate risk for the north and low hazard and risk for the west.



Figure 1.1 Tsunami hazard and risk levels for Northland proposed by Chagué-Goff *et al.*, 2006.

Shortly after this report, Goff *et al.*, (2006) completed their report on tsunami sources relevant to the Northland, Auckland, Waikato and Bay of Plenty regions. This report identified the four most significant tsunami sources relevant to these regions which included sources from South America, the Solomon/New Hebrides region, the TK Trench and selected local sources. This study was pioneering in that they proposed that a large subduction zone earthquake along the TK Trench represented the most significant tsunami source for the region. The modelling presented in this report was done over relatively coarse modelling grids and only produced offshore maximum amplitudes highlighting areas of tsunami amplification. Furthermore, the distant source modelling did not directly model the trans-Pacific propagation, but rather uses a synthetic, ad-hoc time series applied to the eastern boundary of the model domain. As such, the modelling results are quite limited in their applicability.

More detailed modelling was presented in the next report prepared by Lane *et al.*, (2007). This study focused on tsunamis from South America and from the TK Trench and used the same hydrodynamic model as in Goff *et al.*, (2006) but over more detailed bathymetric and topographic grids. As with the previous work, this study has the serious flaw of using an assumed time series imposed along the eastern boundary of the model domain rather than considering the full propagation of the tsunami waves across the Pacific basin. Ultimately this study produced inundation and flow speed maps for several sites in Northland.

This work was carried on in subsequent reports by Gillebrand *et al.*, (2008), Arnold *et al.*, (2009) and Arnold *et al.*, (2011). Each of these studies used the same modelling methodology and tsunami sources as the original Goff *et al.* (2006) and Lane *et al.* (2007) reports. As a result, they all suffer from the same flaw of not properly accounting for the trans-Pacific propagation or inherent variability in tsunamis emanating from distant sources. Furthermore, detailed inspection of the model output at sites such as Tutukaka reveals a distinct underprediction and lack of detail in the assessments of the tsunami current speeds

(see Figure 1.2). As such, while the inundation extents may be valid, the current speed projections from the NIWA reports are called in to question and should not be used for any sort of maritime related hazard assessments.

1.1.2 Other Reports and Studies

Although not specifically focussing on the Northland region, there have been several reports and papers published dealing with the assessment of the New Zealand tsunami hazard from a variety of far-field sources or studies that focus on the northern and eastern coasts of the North Island.

Firstly, Power *et al.* (2007) proposed a methodology for the probabilistic assessment of tsunami runup around New Zealand focussing on tsunamis emanating from South America. This was followed by the work of Power and Gale (2010) who proposed a methodology for the rapid assessment of a tsunami's potential impact based on earthquake magnitude and location. This methodology is to some extent replicated in this study whereby a set of scenario events is used to precompute the tsunami impact at a site of interest. A look up table (or more specifically, an interactive pdf document) is then produced that allows a user to select a scenario and instantly access information describing the tsunami effects. In the Power and Gale (2010) study this was done for a suite of magnitude (M_w) 8.7, 9.0 and 9.3 earthquakes situated around the Pacific Rim with broad-brush hazard levels determined for the entirety of the New Zealand and the Chatham Islands. In this the analysis is carried out to a higher level of detail for several specific sites in the Northland region. Following this, Power *et al.* (2011) investigated the effect of large magnitude earthquake generated tsunamis from the Tonga-Kermadec, Solomon Islands, and New Hebrides Subduction Zones. As with the other studies mentioned above, the tsunami sources featured uniform slip distributions and provided only rough scale projections of offshore tsunami wave heights rather than any detailed assessments of tsunami effects at specific sites.

In the period from 2012 through 2019, Borrero (eCoast) conducted a series of probabilistically informed inundation studies for the Waikato and Bay of Plenty regions. In these studies, he considered the recently released New Zealand probabilistic model while also using tsunami sources based on historical large-magnitude events. This included distant source events based on large South American earthquakes as well as regional and near-source events on the TK Trench which were based on the tsunami source models used to replicate the near-field effects of the 2011 Tohoku tsunami in Japan. What sets this work apart from the studies of Power *et al.* described above, is the effort to replicate historical events, the use of heterogeneous slip distributions for the tsunami source models and the detailed analysis of tsunami wave heights and current speeds on fine-scale grids.

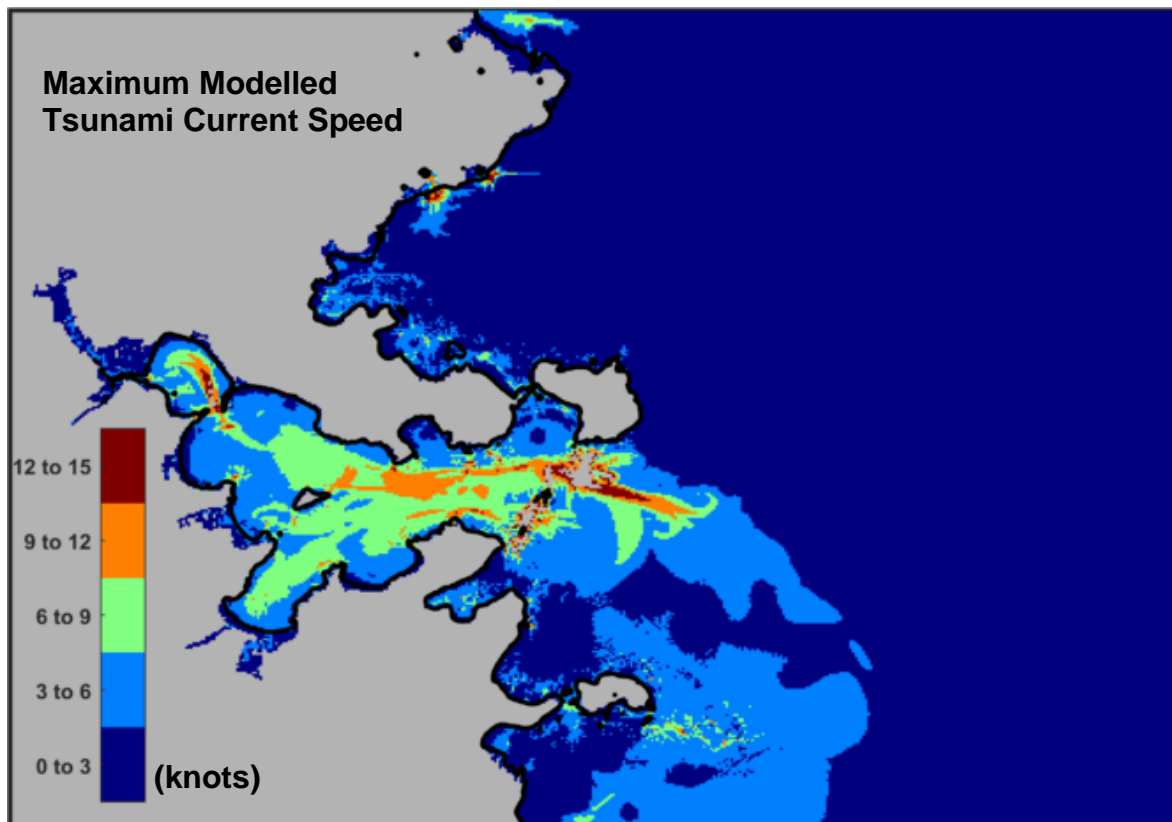
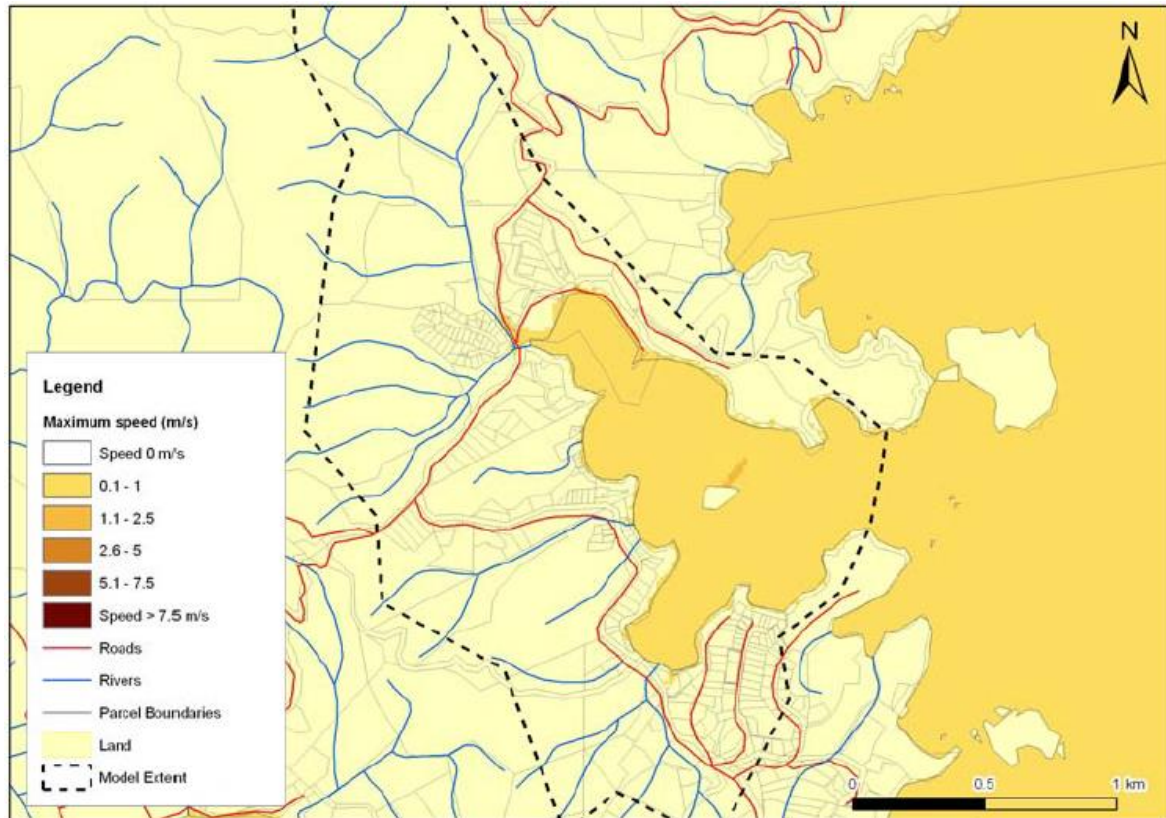


Figure 1.2 Modelled tsunami current speeds at Tutukaka for a large magnitude tsunami from South America representative of the 1868 Arica event. (top) NIWA modelling results. (bottom) results from this study. Note: 1 knot = ~2 m/s.

1.2 Development of Maritime Tsunami Planning Tools and Products

As noted in Borrero *et al.* (2015b), although the tsunami hazard to ports and maritime facilities is well known and has been described countless times in the historical record, it was not until after the trans-oceanic tsunamis of the early 21st century that port-specific warning and response information began to be developed for practical application. This was due in large part to the observations reported by Okal *et al.* (2006 a, b, c) of tsunami currents affecting far-field ports in the Indian Ocean during the 2004 tsunami.

These findings were then reinforced by the detailed investigation of tsunami damage to port infrastructure and effects on maritime activities reported by Dengler *et al.* (2008) following the November 2006 tsunami originating in the Kuril Islands that strongly affected Crescent City, California.

Ports in California were again affected by a distant source tsunami following the February 2010 earthquake in Maule, Chile (Fritz *et al.*, 2011). where strong and damaging currents swamped boats and generated standing waves with effects persisting for many hours after the tsunami arrival (Wilson *et al.*, 2012). In 2011, the Tohoku, Japan earthquake generated a tsunami that again affected ports and maritime facilities across the Pacific with some of the strongest effects again observed in Crescent City, CA (Admire *et al.*, 2014).

Borrero and Greer (2012) conducted a comparative study of the Chile and Japan tsunamis describing the relative effects of these two events in New Zealand and California. noting that the effects of the 2011 Tohoku tsunami in California are analogous to a large tsunami from South America affecting New Zealand with the orientation and distance between the Japanese Subduction Zone relative to California roughly similar to the location and orientation of the South American Subduction Zone to New Zealand.

Based on the observed effects and data collected during the 2004, 2010 and 2011 events. Lynett *et al.* (2012, 2014) developed tools and methodologies for the robust assessment of tsunami induced current hazards in ports and marinas. This work was conducted concurrently with efforts in New Zealand and the results were applied to both California (Kalligeris *et al.*, 2016, Ayca and Lynett, 2016, Kalligeris *et al.*, 2017, Wilson *et al.*, 2017, Keen *et al.*, 2017) and New Zealand (Borrero *et al.*, 2014, Borrero and Goring, 2015) with these last two studies laying the groundwork for the work presented in this report.

In Appendix 1 we reproduce a portion of a report by Borrero *et al.* (2014) that details some of the effects seen in ports and harbours in the Indian and Pacific Oceans as a result of the distant source tsunamis of 2004 (Sumatra, Indonesia), 2008 (Kuril Islands), 2010 (Maule, Chile) and 2011 (Tohoku, Japan).

1.3 Study Sites

The Northland Region of New Zealand is an ideal area to conduct a maritime tsunami hazard assessment. The area is popular amongst recreational boaters and has an active commercial fishing fleet. There are numerous small marinas and hundreds of mooring sites scattered across the area. Dozens of cruise ships call in to the Bay of Islands each year, mooring offshore and ferrying guests ashore with small launches. In addition, Marsden Point is the site of a large commercial port (Northport) that exports a large volume of forestry products. Northport is located near two oil jetties that are operated by the New Zealand Refinery Company and another jetty operated by Golden Bay Cement which is used to transport products from the Portland Cement Plant (Popovich, 2015). In terms of tsunami hazard, the region is vulnerable to near, regional and distant source tsunamis and has been affected by multiple events over recorded history. The TK Trench represents a significant hazard to the Northland region as it faces a nearly 600 km long subduction zone segment that would focus any tsunami energy directly towards its shores.

We have selected six sites for detailed analysis. These include Whangaroa, Doves Bay, Waitangi/Paihia, Opuia, Tutukaka and Marsden Point as shown in Figure 1.3. Detailed Information about the maritime facilities present at each site are presented in Appendix 1.



Figure 1.3 Location map for study sites and other locations mentioned in the text.

2 HISTORY OF TSUNAMIS AFFECTING NORTHLAND

Northland has been affected by numerous tsunamis in historical times and there is evidence of tsunami affecting the area in prehistoric times.

2.1 Prehistoric Tsunami Records

The New Zealand Palaeotsunami Database. (NZPTB, 2017) contains numerous records of evidence pointing to the occurrence of a palaeotsunami affecting the coast of Northland. Some of this data was originally reported in the work of Chagué-Goff and Goff (2006) and Goff *et al.* (2010a, b) among others. In Figure 2.1 we reproduce an image from the NZPTB website showing the location of palaeotsunami evidence. This figure suggests that substantial evidence exists for the occurrence of significant palaeotsunamis having affected the Northland coastline.

Goff *et al.* (2010a) describe the available data in more detail and ascribe the data points to three separate events. The oldest of these events are believed to have occurred approximately ~6500, ~2800 years before present (BP) and are associated with possible large magnitude earthquakes on the TK Trench. The most recent of the three events was dated to 1450 AD (569 years BP), however no clear source for this event has been determined. Goff *et al.* (2010a) tentatively associate it with the eruption of the Kuwae Caldera in 1452/1453 AD.

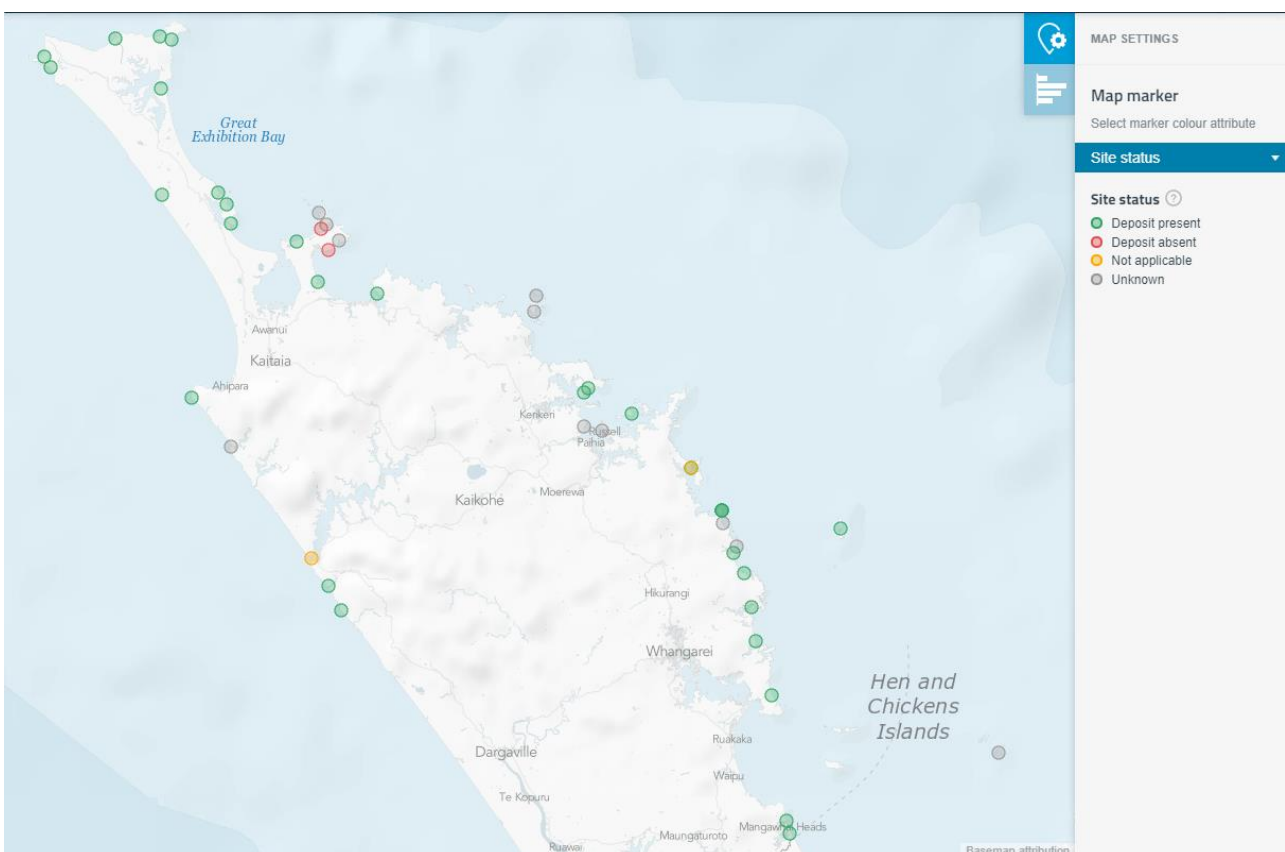


Figure 2.1 Locations of prehistoric tsunami deposits or evidence in Northland.

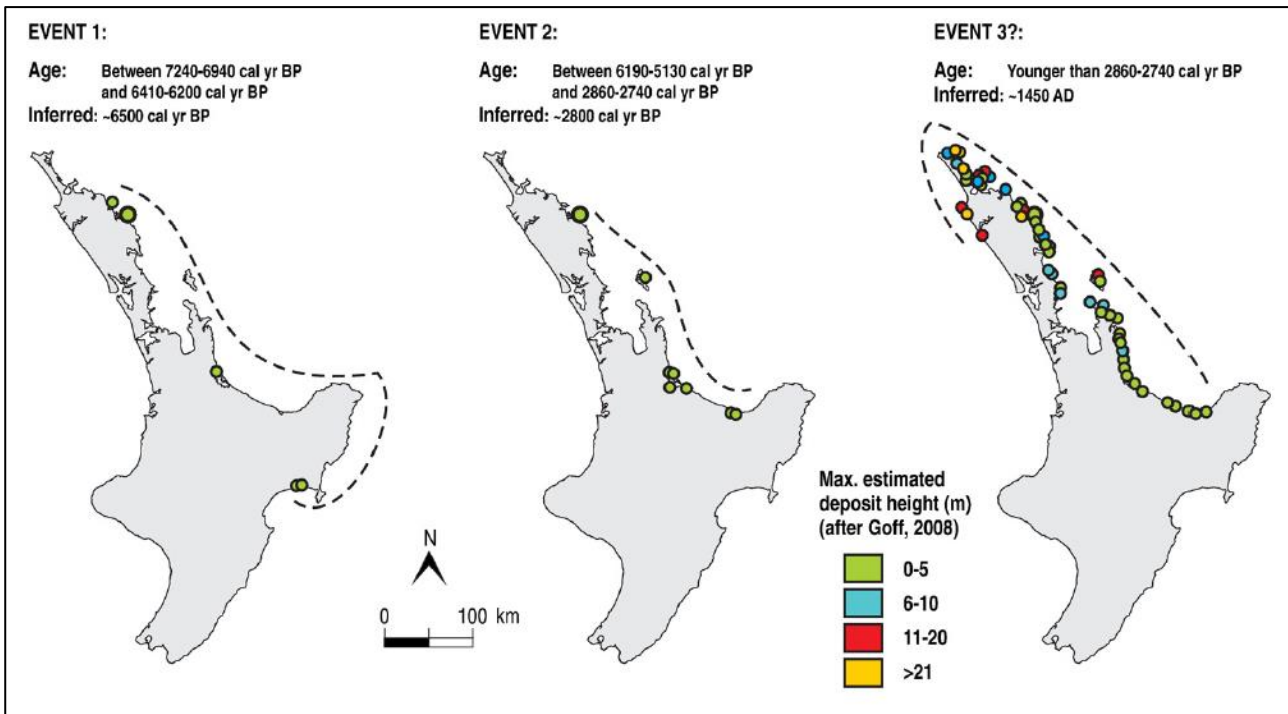


Figure 2.2 The locations of evidence related to three separate prehistoric tsunami events believed to have affected Northland (from Goff *et al*, 2010a)

2.2 Historic Tsunami Records

There are numerous accounts of tsunamis affecting Northland in the historical record. In Table 2.1 we summarise these accounts collected from De Lange and Healy (1986) and from GNS’s on-line historical tsunami database (Downes *et al.*, 2017, GNS, 2018). Of these, all are distant source events other than the 1976 Kermadec Island event which was a regional event.

Besides the events listed below, the Northland Region was also affected by the February 2010 Maule Chile tsunami and the 11 March 2011 Tohoku, Japan tsunami (GNS Database, Borrero and Greer, 2012, Borrero *et al.*, 2012). The available complete and detailed descriptions of the effects of the different tsunami events at locations in the Northland Region are reproduced in Appendix 2.

Of the events listed below, the 1877 and 1960 events from northern and southern Chile respectively are the most thoroughly described with strong effects observed and or recorded in Tutukaka and the Bay of Islands area. It is interesting to note that the 1877 event seems to have been larger – or at least more widely noticed - than the 1868 event although the 1868 event is generally regarded to have been a ‘bigger’ tsunami. However, we note that given the relatively sparse population of New Zealand in the mid 1800’s and inconsistencies in data collection and reporting, all of the tsunami data recorded prior to the 1970’s should be treated with caution.

Table 2.1 Summary of some historical tsunami events and effects in Northland.

Site Name	Tsunami Height (m)	Inundation depth (m)	Note
1835 Central Chile			
Waitangi			reported
1868 Southern Peru, 13 August, 21:30 UTC			
Doves Bay	1.2	0.6	
Mangonui	1.2-1.5		
Russel	n/a		above spring high tide.
1877 Northern Chile, 10 May, 00:59 UTC			
Waitangi	1.8, 3.0		Large tidal wave into the bay, 3.0 m reported by Laing (1954), tender from 'Iona' swept above the high tide mark
Tutukaka		1.6	Several waves came in each succeeding wave decreasing in size/force
Russel	1.8		The tide ebbed and flowed seven times on May 11. Max. fluctuation of 1.8 m
Paihia	3.1, 3.6(?)		Mid-day May 11th, water dropped 1.2 m then rose 1.9 m by 12:25 pm. 'Gazelle' grounded in water depth of 3.6 m
Wairoa Bay	n/a		4 pm, May 11th, wave rushed in and flooded 9 m (laterally) above high-water mark. Two boats washed ashore and left high and dry in a paddock
Bay of Islands (various)	2.5		Reports from islands within the bay of sudden rise of 2.5 m around 5 pm on May 11th, followed by ebbing and flowing every 20 min.
1946 Aleutian Islands 1 April, 12:28 UTC			
Tutukaka	0.6	1.2	waves in rapid succession occurring for several days
Tutukaka	0.3-0.5		0.3 m bore observed on the river at 7:30 pm on the 5th of November followed by 'tidal fluctuations' of about 0.5 m
1952 Kamchatka, 4 November, 16:58 UTC			
Tutukaka	0.75		
1960 Chile, 22 May, 19:11 UTC			
Mangonui	1.2		1.2 m rise and fall was recorded within 10 minutes. A submarine telephone cable was broken on the 24th.
Whangaroa			Boat left "high and dry"
Waitangi	n/a		Strong flood and ebb flows at 20-40 min intervals starting late on 23rd May. Whirlpools observed, one boat damaged following a collision with the Waitangi Bridge.
Opuia	1-1.5	1.5	water level changed 3-4ft in minutes, formation of whirlpools
Opuia	3.0		Reports are similar to those from Waitangi, flashing channel marker beacon was damaged when strong flows broke a supporting pile. Boats moored in 3 m of water were grounded.
Tutukaka	2.8	1.5	water receded then returned, rising 2.8 m within minutes. Surges continued at 15-30-minute intervals. Coast road flooded and a bridge abutment damaged.
Whangarei	1		A series of 1 m swells were reported from the Town Basin.

Marsden Point		2	no damage
1964 Alaska March 28, 03:36 UTC			
Whangaroa	1		Boat left "high and dry"
Waitangi		0.6	10 knot tides
Opuā			10 knot tides
Marsden Point	0.3	0.3	1ft variation in tide
1976 Kermadec Islands, 15 January, 07:10 UTC			
Tutukaka	0.2	0.75	0.2m rise lasting 5-6 minutes came in as a "big whirlpool"
Tutukaka	0.75		Sudden surge of 0.75 m. Several yachts damaged when one broke its moorings and was swept in to the others in the harbour. Wave arrived about 3 hours after the earthquake.
1977 Tonga, 22 June, 22:09 UTC			
Opuā	0.15	0.15	
1994 Kuril Islands, 4 October, 13:23 UTC			
Marsden Point	0.1		
2001 Southern Peru 23 June, 20:34 UTC			
Marsden Point	0.18		
2006 Tonga 3 May, 15:27 UTC			
Marsden Point	0.15		
2010 Maule, Chile, 27 February, 18:34 UTC			
Numerous accounts throughout Northland, +/- 0.2 m on Marsden Point tide gauge (see Section 4.1 of this report), also see GNS database and Borrero and Greer (2012) for more details.			
2011 Tohoku, Japan, 11 March, 05:46 UTC			
Numerous accounts throughout Northland, +/- 0.3 m on Marsden Point tide gauge (see Section 4.2 of this report), also see GNS database, Borrero <i>et al.</i> , (2012) and Borrero and Greer (2012) for more details.			

3 MODELLING APPROACH

The numerical modelling presented in this study was carried out using the Community Model Interface for Tsunamis (ComMIT) numerical modelling tool. The ComMIT model interface was developed by the United States Government National Oceanic and Atmospheric Administration's (NOAA) Centre for Tsunami Research (NCTR) at the Pacific Marine Environmental Laboratory (PMEL) following the December 26, 2004 Indian Ocean tsunami as a way to efficiently distribute assessment capabilities amongst tsunami prone countries.

The backbone of the ComMIT system is a database of pre-computed deep-water propagation results for tsunamis generated by unit displacements on fault plane segments (100 x 50 km) positioned along the world's subduction zones. Currently, there are 1,691 pre-computed unit source propagation model runs covering the world's oceans included in the propagation database. Using linear superposition, the deep ocean tsunami propagation results from more complex faulting scenarios can be created by scaling and/or combining the pre-computed propagation results from a number of unit sources (Titov *et al.*, 2011). The resulting trans-oceanic tsunami propagation results are then used as boundary inputs for a series of nested near shore grids covering a coastline of interest. The nested model propagates the tsunami to shore computing wave height, velocity and overland inundation. The hydrodynamic calculations contained within ComMIT are based on the MOST (Method Of Splitting Tsunami) algorithm described in Titov and Synolakis (1995, 1997) and Titov and Gonzalez (1997). The ComMIT tool can also be used in conjunction with real time recordings of tsunami waveforms on one or more of the deep ocean tsunameter (DART) stations deployed throughout the oceans to fine tune details of an earthquake source mechanism in real time. An iterative algorithm that selects and scales the unit source segments is used until an acceptable fit to the observed DART data is met (Percival *et al.*, 2010).

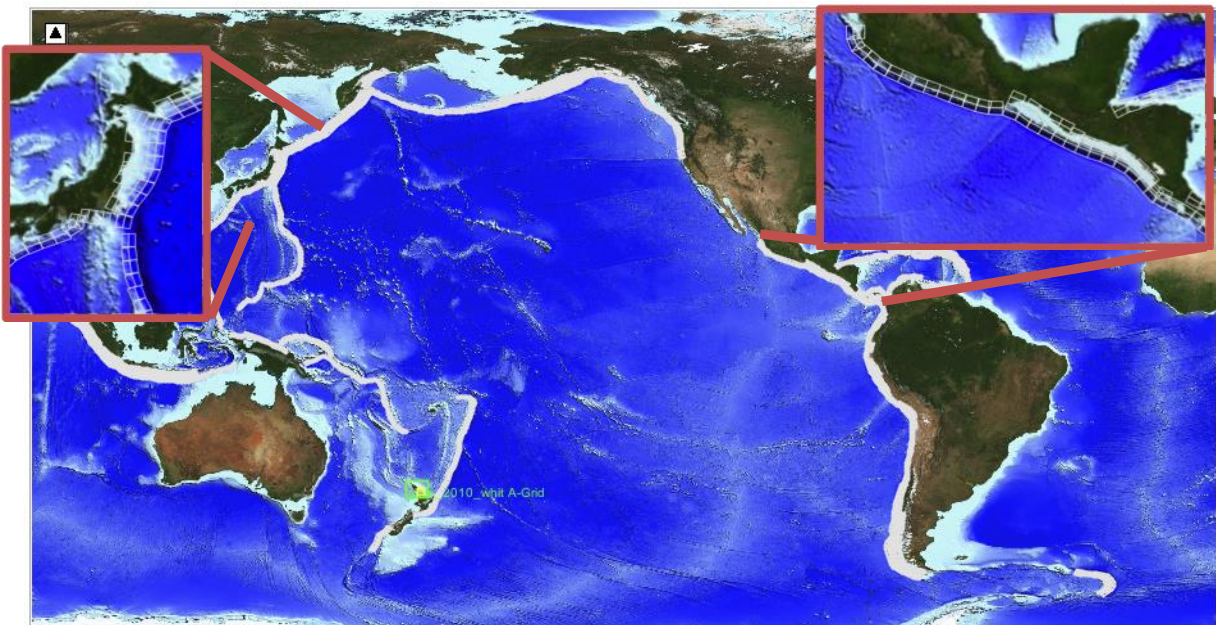


Figure 3.1 The ComMIT propagation model database for tsunamis in the world's oceans. Insets show the details of the source zone discretization into rectangular sub-faults.

3.1 Using ComMIT to Model Tsunami Currents

The MOST/ComMIT algorithm and framework has been used numerous times to accurately model tsunami induced wave height and current speeds. Firstly, Lynett *et al.* (2014) showed that the MOST/ComMIT tsunami model accurately reproduced measured tsunami current speeds in Crescent City California caused by the 2011 Tohoku tsunami. Furthermore, they showed that the MOST/ComMIT results were comparable in terms of magnitude and spatial extent to higher order Boussinesq models (Figure 3.2).

This contrasts with the COMCOT model which was shown by Son *et al.* (2011) to be unable to reproduce complex tsunami currents inside the Port of Salalah, Oman during the 2004 Indian Ocean tsunami. They attributed this shortcoming in COMCOT to the numerical truncation error of the upwind differencing in COMCOT which manifests as a diffusion term in COMCOT's governing equations resulting in an overall underprediction of tsunami current speeds. Later, Borrero (2017) showed that the MOST/ComMIT model was able to reproduce the complex current patterns, including the formation of large scale eddies inside the port, observed at Salalah during the 2004 tsunami event (Figure 3.3).

This is an important point since the COMCOT model is used by GNS for tsunami impact studies in New Zealand. While COMCOT is known to behave comparably to MOST/ComMIT (and many other models) for the prediction of water surface elevation and inundation extents, it has also been shown to be deficient in its ability to predict complex, tsunami induced currents.

Additionally, as shown previously in Section 1.1.1 and Figure 1.2, the modelling approach used by NIWA in their studies of tsunami effects in Northland produced current speed predictions that are noticeably deficient in the magnitude and extent of tsunami induced current speeds.

Specific to New Zealand, data of current speeds recorded in Tauranga Harbour during the 2011 Japan tsunami was accurately reproduced by Borrero *et al.* (2015) using the MOST/ComMIT model (Figure 3.4). Careful inspection of Figure 3.4 shows that the deficiencies in the MOST/ComMIT current speed output occur in the portion of the record where the tsunami height is under predicted. Borrero *et al.* (2015) attributes this mismatch to deficiencies in the source model used to initialise the tsunami propagation model and not specifically to any shortcoming in the MOST/ComMIT algorithm itself since the measured current speeds are well reproduced when the modelled tsunami heights match the measured data.

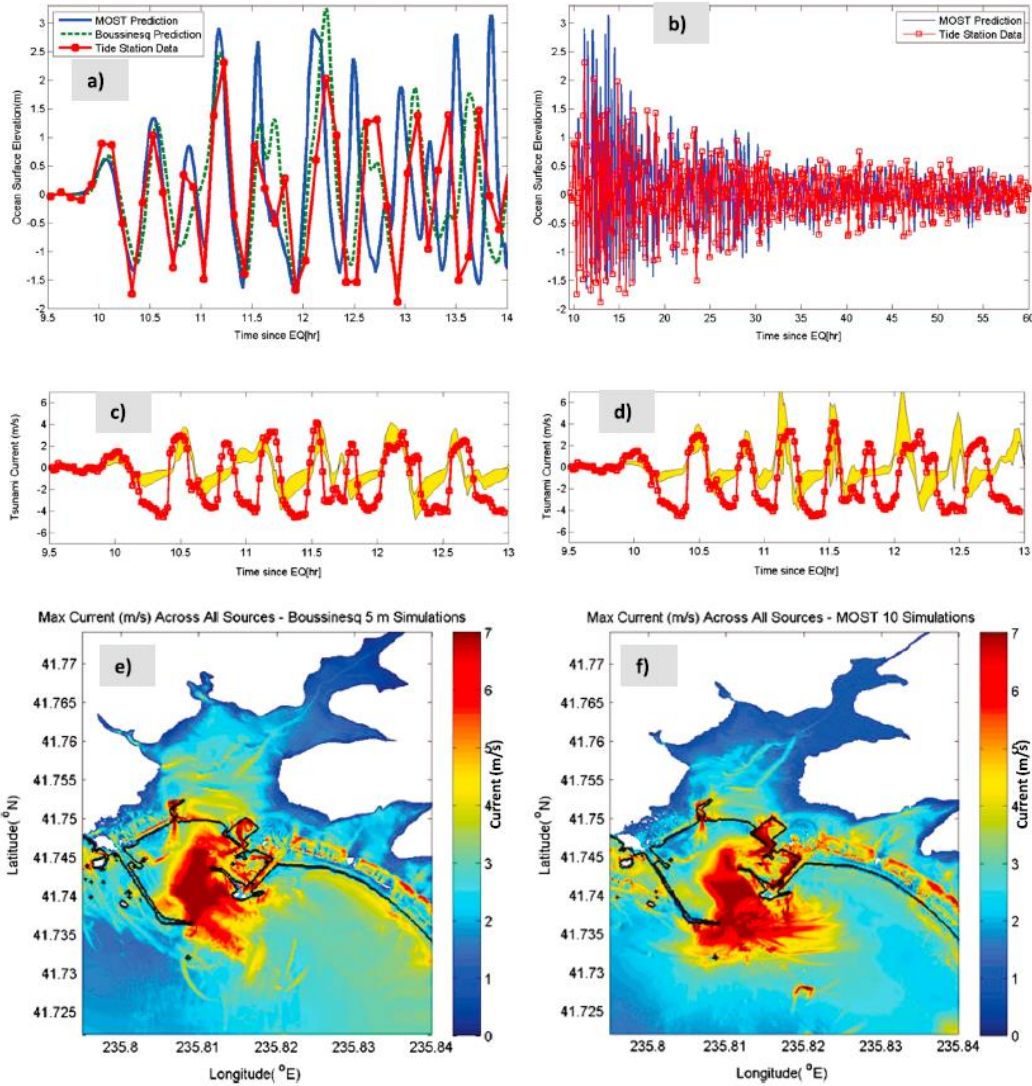


Figure 3.2 Validation and comparison of numerical simulation tools for water surface elevation and currents in Crescent City, CA; (a) comparison of MOST (blue solid), Boussinesq (green dashed), and tide station data (red solid + dots) for the 2011 Tohoku tsunami; (b) comparison of MOST (blue solid) and tide station data (red solid + dots) for 60 h post-EQ; (c) comparison of fluid speed (m/s) at inner boat basin entrance between Boussinesq (yellow) and digitized video data (red solid + dots); (d) comparison of fluid speed (m/s) at inner boat basin entrance between MOST (yellow) and digitized video data (red solid + dots); (e) maximum speed predicted by COULWAVE across a range of different tsunami sources; and (f) maximum speed predicted by MOST across a range of different tsunami sources. (reproduced from Lynett *et al.*, 2014).

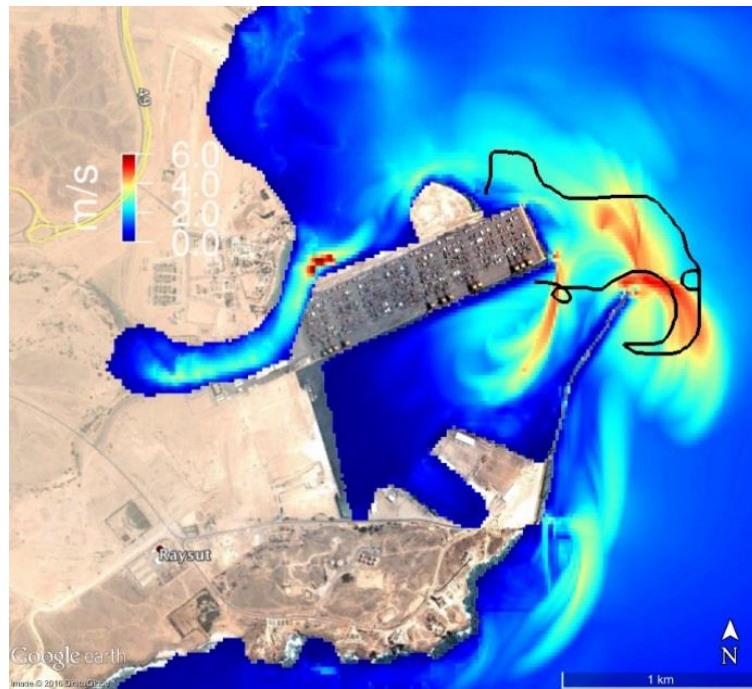


Figure 3.3 Modelled maximum tsunami current speeds at the Port of Salah during the 2004 Indian Ocean tsunami. Black trace represents the estimated path of the Maersk Mandraki container ship as it drifted through port after it was torn from its mooring by the tsunami currents (see Okal *et al*, 2006b). Figure reproduced from Borrero, 2017.

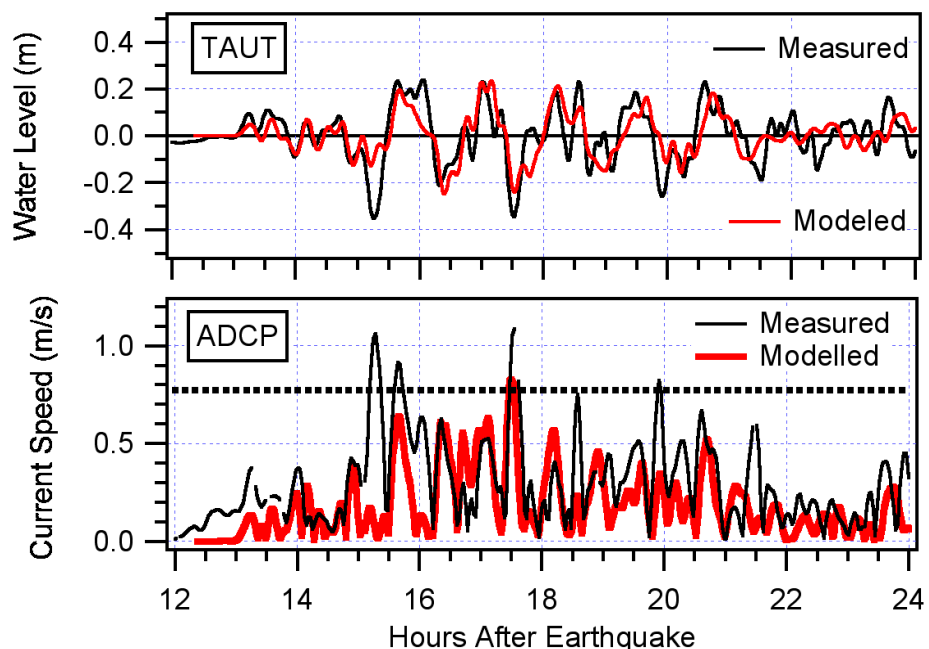


Figure 3.4 Modelled vs. measured tsunami heights (top) and current speeds (bottom) from the 2011 Japan tsunami at the entrance to Tauranga Harbour using the MOST/ComMIT model. Figure reproduced from Borrero *et al.*, 2015.

3.2 A Note on Terminology

There is often some ambiguity in the terminology used to describe the size of a tsunami. Generally, the term ‘height’ is used as defined in the figure above, i.e. the measure of a distance above a particular datum. However, since tsunamis are waves, it is also common to use the term ‘amplitude’ which is the distance (height?) above or below a particular datum. For a perfectly symmetrical sine wave, the ‘height’ is twice the ‘amplitude’.

In Power (2013) he writes:

“TSUNAMI HEIGHT (m) is the vertical height of waves above the tide level at the time of the tsunami (offshore it is approximately the same as the AMPLITUDE). It is far from constant, and increases substantially as the wave approaches the shoreline, and as the tsunami travels onshore. The term “WAVE HEIGHT” is also often used, but there is a potential ambiguity as many scientists define WAVE HEIGHT as the peak-to-trough height of a wave (approximately twice the amplitude). Note that this is a change in terminology from the 2005 Tsunami Hazard and Risk Review, intended to bring greater consistency with international usage of these terms.

And with regards to runup he says:

“TSUNAMI RUN-UP (m), a measure much used in tsunami-hazard assessment, is the elevation of inundation above the instantaneous sea level at the time of impact at the farthest inland limit of inundation. This measure has a drawback in that its relationship with the amplitude of the waves at the shore depends markedly on the characteristics of waves and on the local slopes, vegetation, and buildings on the beach and foreshore areas, so it is highly site-specific.”

And finally, with regards to the hazard curves for the National Tsunami Hazard Model he writes:

“in the curves shown here the ‘maximum amplitude’ should be interpreted as the tsunami height measured at the location within the section where it is highest”

Hence there is a degree of interchangeability in the use of ‘height’ and ‘amplitude’. In this report we use ‘height’ for the elevation of the water surface above the sea level datum at the start of a model run. When discussing the hazard curves, we use the term ‘amplitude’ in line with Power (2013), which, as we see above, is used interchangeably with ‘height’.

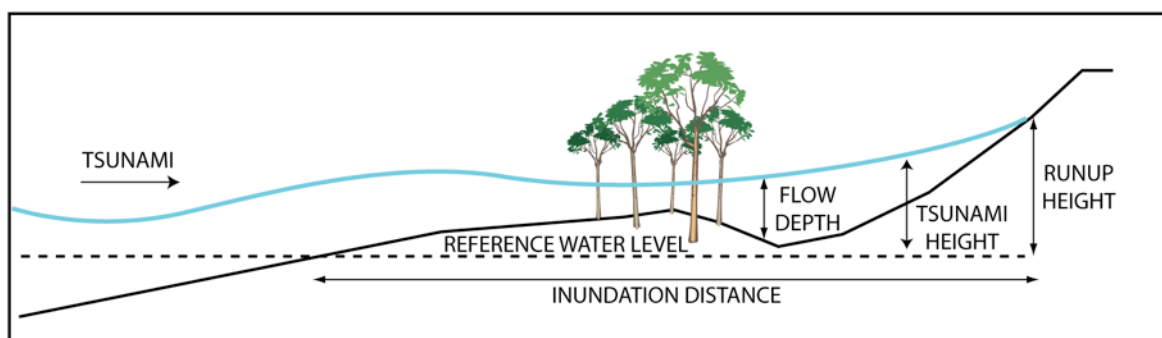


Figure 3.5 Definition sketch for tsunami height, flow depth, runup and inundation distance.

3.3 Numerical Modelling Grids

The Northland Regional Council provided LiDAR topography data for construction of the numerical modelling grids. This data was combined with additional data sets covering the regional offshore bathymetry and on land topography. This included the Shuttle Radar Topography Mission (SRTM) 90 m resolution topography, 200 m resolution bathymetry from NIWA, as well as hydrographic chart data from Land Information New Zealand (LINZ). The data were combined into a master set of (x, y, z) triplets and then gridded into different resolutions and coverage areas using the Kriging algorithm from the Surfer software package. Model grids were set up for mean sea level (MSL). Each model run utilized the same A grid, but the areas studied were divided into 4 different B grids for modelling. Details for each of the model grids used in this study are presented in Table 3.1, the orientation and location of the A, B and C-level grids is shown in Figure 3.6 and Figure 3.7. Filled contour plots of the individual grids are presented in Appendix 4.

Table 3.1 The details of the various computational grids.

	dx (m)	dy (m)	nx (nodes)	ny (nodes)	max. dt (seconds)
A (regional)	2500	2400	328	227	11.33
B0 (Whangaroa)	100	100	501	428	1.20
C0 (Whangaroa Entrance)	10	10	228	214	0.62
C1 (Whangaroa Marina)	10	10	119	175	0.92
B1 (Bay of Islands)	100	100	501	389	2.06
C2 (Doves Bay)	10	10	228	167	0.71
C3 (Waitangi/Paihia)	10	10	318	245	0.92
C4 (Opuā)	10	10	228	278	0.66
B2 (Tutukaka)	100	100	546	389	2.18
C5 (Tutukaka)	10	10	454	389	0.42
B3 (Marsden)	150	150	362	297	4.02
C6 (Marsden Point/Northport)	10	10	635	556	0.54

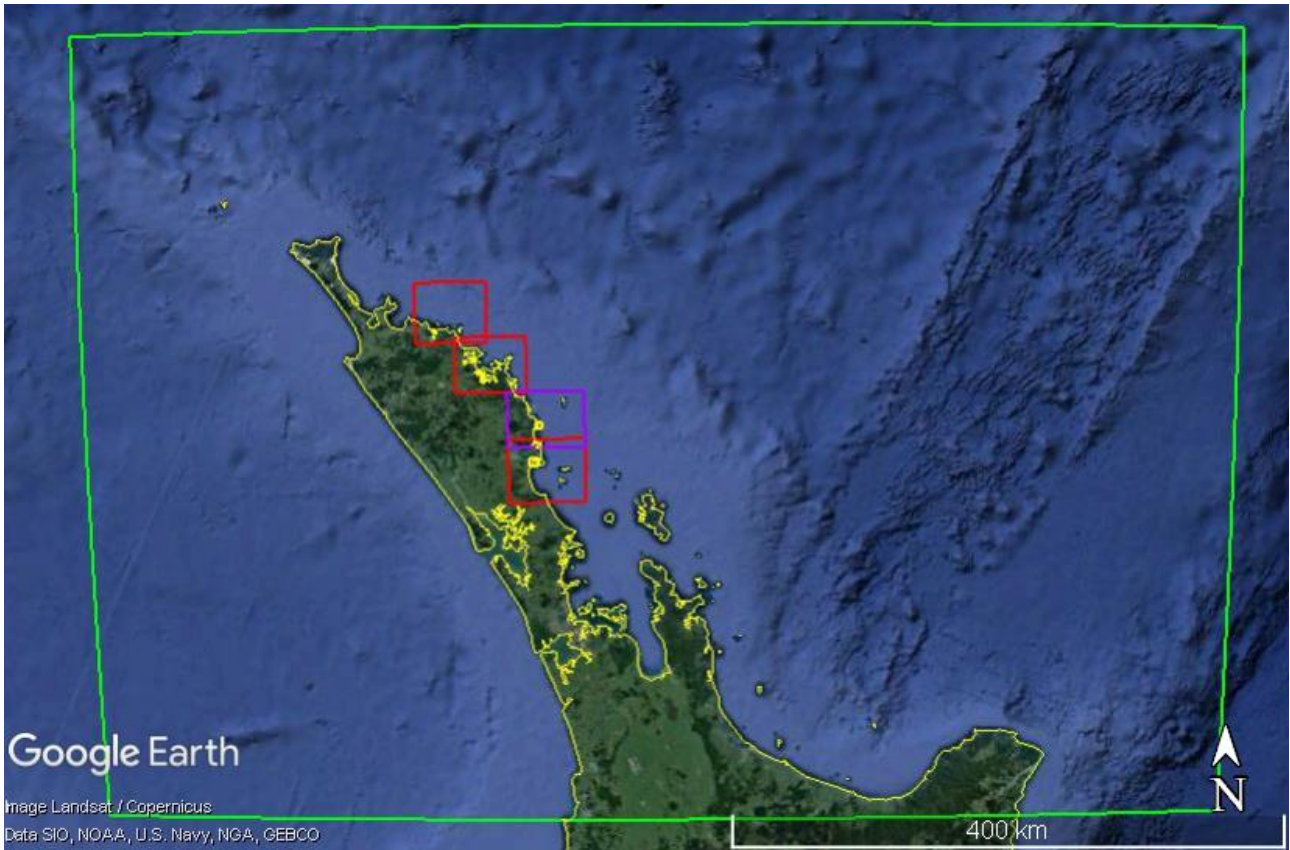


Figure 3.6 Extents of the A level (green) and B level (red) grids.



Figure 3.7 Extents of the B level (red) and C level (yellow) grids.

3.4 Tsunami Sources

This study focuses on tsunamis generated by large magnitude (M_w 8.7, 9.0 and 9.3) subduction zone earthquakes. Therefore, we model from source, a suite of earthquake scenarios at these magnitudes positioned at 72 different locations around the Pacific rim. The sources are separated into groups by region and spaced some 500-600 km apart as shown in Figure 3.8.

Each tsunami scenario is initialised using the unit sources in the ComMIT database. For the 8.7 and 9.0 sources we used a 500 x 100 km fault area (i.e. a 5 x 2 cluster of fault segments) while for the 9.3 scenarios this was extended by 200 km to a 900 x 100 km fault plane (9 x 2 fault segments).

The slip distribution for each source was non-uniform with more slip applied to the deeper segments. This was done based on the work of Power *et al.* (2015) who showed, using the ComMIT model, that for South American sources affecting Marsden Point in Northland, increasing the slip on the deeper segments results in larger tsunami heights at the port. We applied this type of slip distribution to provide conservative estimates of the potential tsunami effects from each source region. The specific slip amounts for each source magnitude are listed in Table 3.2 below.

Table 3.2 Slip amounts (in meters) applied to each segment in the sensitivity study.

M 8.7		M 9.0		M 9.3	
deep	shallow	deep	shallow	deep	shallow
-	-	-	-	40.5	15.6
-	-	-	-	40.5	15.6
11.0	4.2	26.0	10.0	40.5	15.6
11.0	4.2	26.0	10.0	40.5	15.6
11.0	4.2	26.0	10.0	40.5	15.6
11.0	4.2	26.0	10.0	40.5	15.6
11.0	4.2	26.0	10.0	40.5	15.6
-	-	-	-	40.5	15.6
-	-	-	-	40.5	15.6

As noted in Power and Gale (2010), “one drawback of pre-calculated model scenarios is that any actual event is unlikely to precisely match any one scenario. The location will in general not correspond exactly to one of the scenarios, and in most cases the magnitude will have to be rounded up to the nearest modelled magnitude, or the model results subject to empirical scaling. Even with a close match to location and magnitude there are other factors, such as the earthquake depth and detailed slip-distribution, that affect the scale of the tsunami generated.”

This is of course true, however the products developed here (and in Power and Gale 2010 and Borrero *et al.*, 2014) are intended for use as an initial assessment of the tsunami threat which can then be refined as more information becomes available.

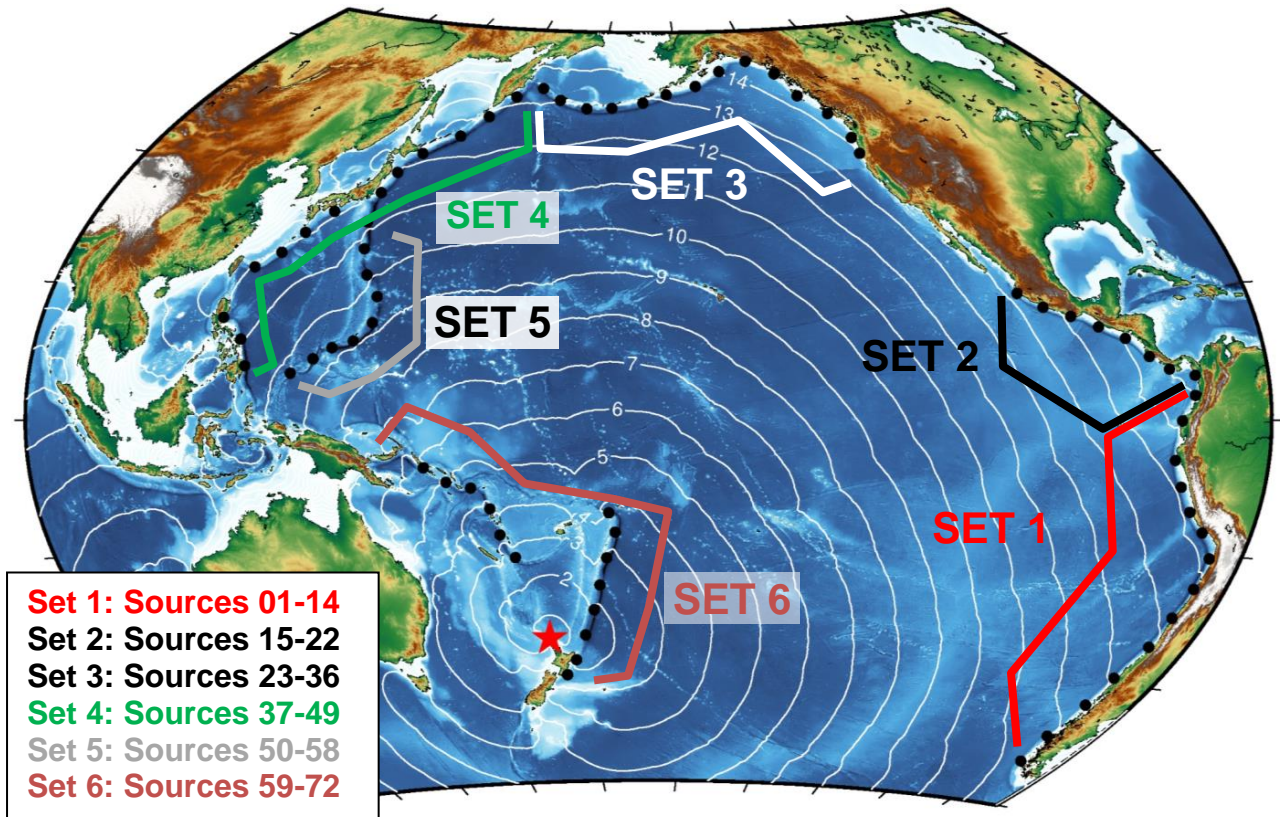


Figure 3.8 Tsunami source regions for the tsunami modelling.

3.5 Tsunami Travel Times

In Figure 3.9 we present tsunami travel time contours to Northland. These travel times were computed using the ‘TTT’ software which calculates the speed of propagation of a shallow water wave across variable bathymetry using Huygens’ method (Shokin *et al.*, 1987). Rather than determining the travel time from each source to Northland, we plotted the travel times from Northland outward. Plotting the data this way gives a clear indication of the number of hours from any point in the Pacific Ocean to Northland. Note however, that this is a *minimum* arrival time, i.e. this is the fastest possible time that a tsunami could cross from its source location to Northland. Also, observed difference between predicted and actual travel times is due to a combination of factors including inaccuracies in the bathymetry and nonlinear propagation effects. Also, it is important to remember that ‘first arrival’ is not when the strongest tsunami effects occur. For distant source tsunami in particular, the strongest effects generally occur many hours after first arrival. We have accounted for this in this study by plotting the computed water level time series in the detailed model domain and noting the timing of the highest and lowest water levels. This is discussed in more detail in Section 6.1.

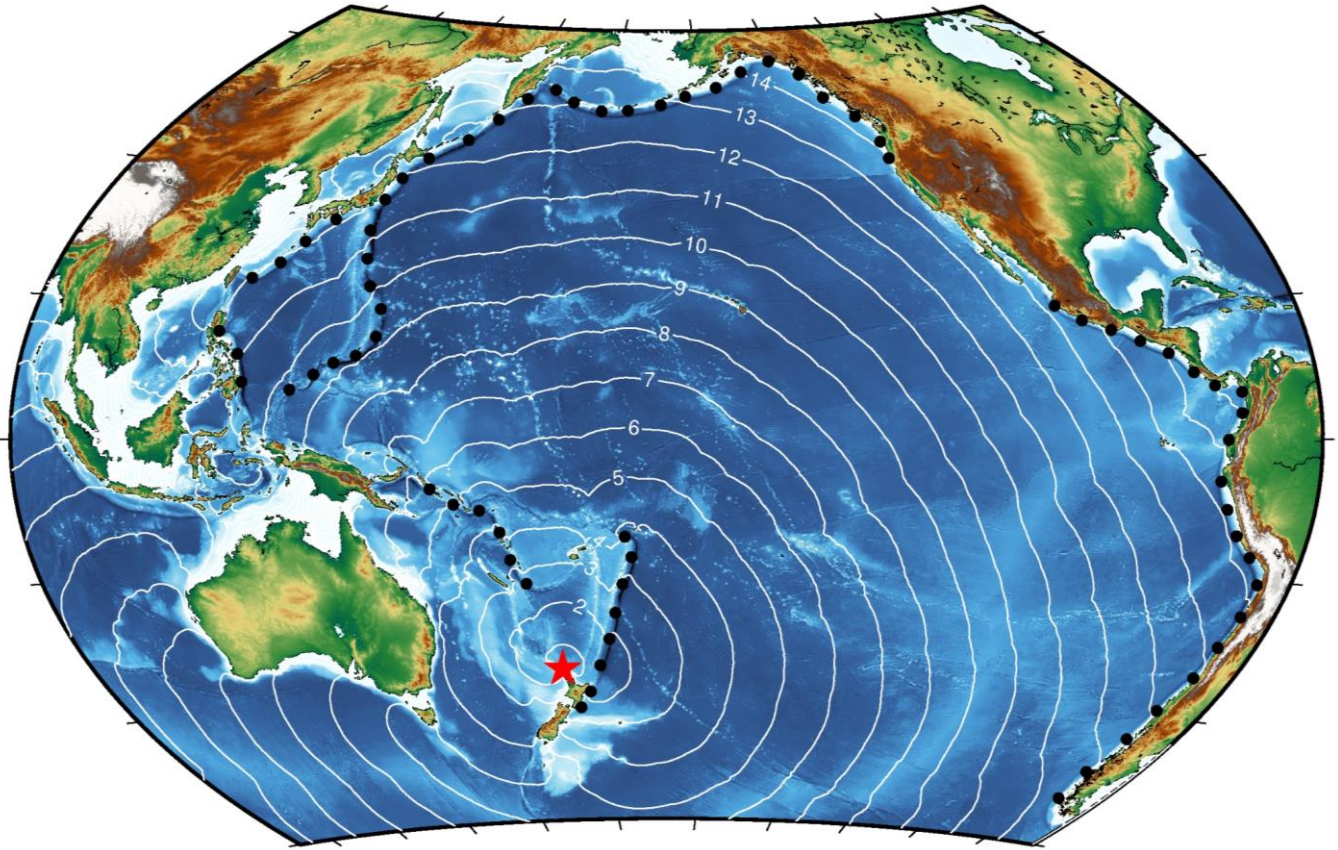


Figure 3.9 Tsunami travel times to Northland (red star). The 72 source locations are shown with black dots while the tsunami travel times are shown as white contours.

4 VALIDATION OF THE COMMIT MODEL TSUNAMIS AFFECTING NORTHLAND.

The ComMIT model has been validated for both distant source and near source events. In the following sections we present results showing the performance.

4.1 Case 1: The February 27, 2010 Maule, Chile Earthquake and Tsunami

For the 2010 Maule Chile event we used the tsunami source model developed by NOAA for use within the ComMIT system. This source is shown in Figure 4.1 below along with the resultant trans-Pacific propagation pattern of the maximum tsunami amplitude. We compared the model output to water levels recorded at Marsden Point as this is the only site in the study area with available tide gauge data from a tsunami event. The model to measured comparison is presented in Figure 4.2 and shows a good fit in terms of arrival time, wave shape and amplitude between the measured and model result.

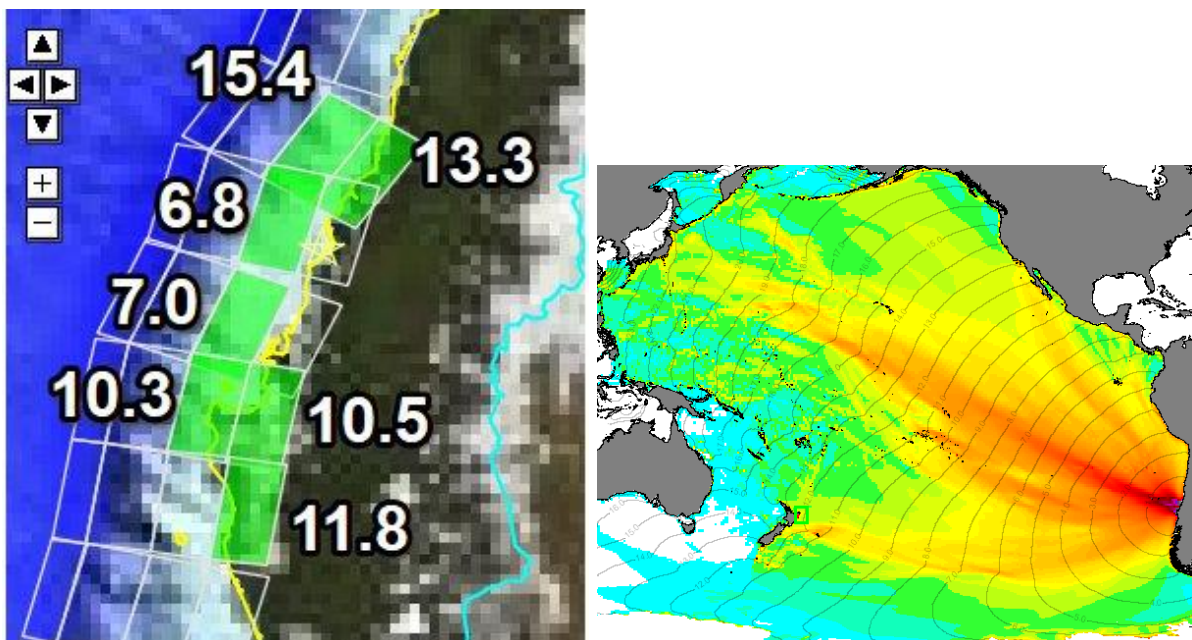


Figure 4.1 Tsunami source model (left) and the trans-pacific propagation pattern (right) for the 2010 Maule, Chile tsunami. Slip amounts (in meters) for the individual fault segments are indicated in white.

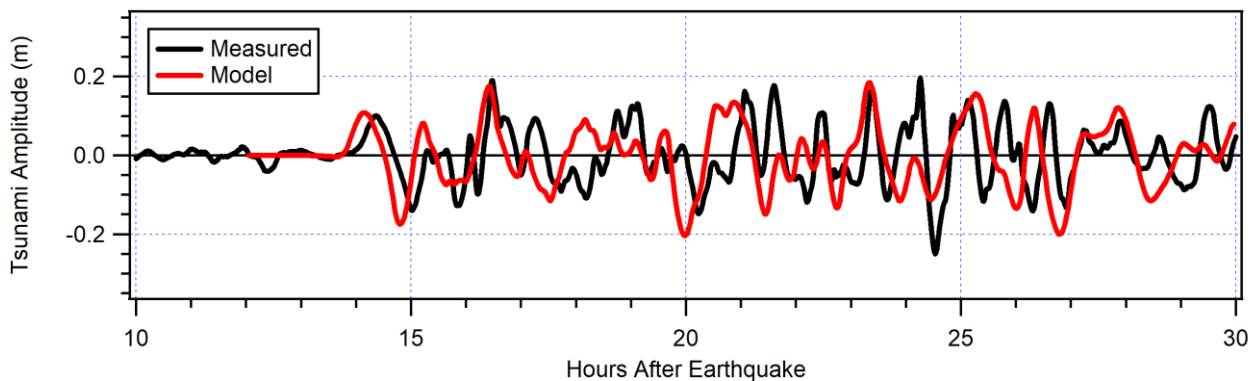


Figure 4.2 Modelled water level time series compared to measured data at the Marsden Point tide gauge for the 2010 Maule, Chile tsunami.

4.2 Case 2: The March 11, 2011 Tohoku Earthquake and Tsunami

The March 11, 2011 Tohoku earthquake and tsunami also presents an excellent case study for the validation of the ComMIT model. The tsunami event was recorded on tide gauges throughout New Zealand with a wealth of data recorded on five water level gauges and one current meter in Tauranga Harbour (Lynett *et al.*, 2012, Borrero *et al.*, 2012, Borrero and Greer 2013) with the effects there modelled in Borrero *et al.*(2015).

As with the 2010 event, here we compare the model results to data recorded on the Marsden Point tide gauge. Also, as with the Chile event, the model was initialised using the tsunami source developed by NOAA for use within the ComMIT modelling system (see Figure 4.3). The model results (Figure 4.4) show a good fit to the measured data in terms of arrival time, wave form and amplitude at Marsden Point.

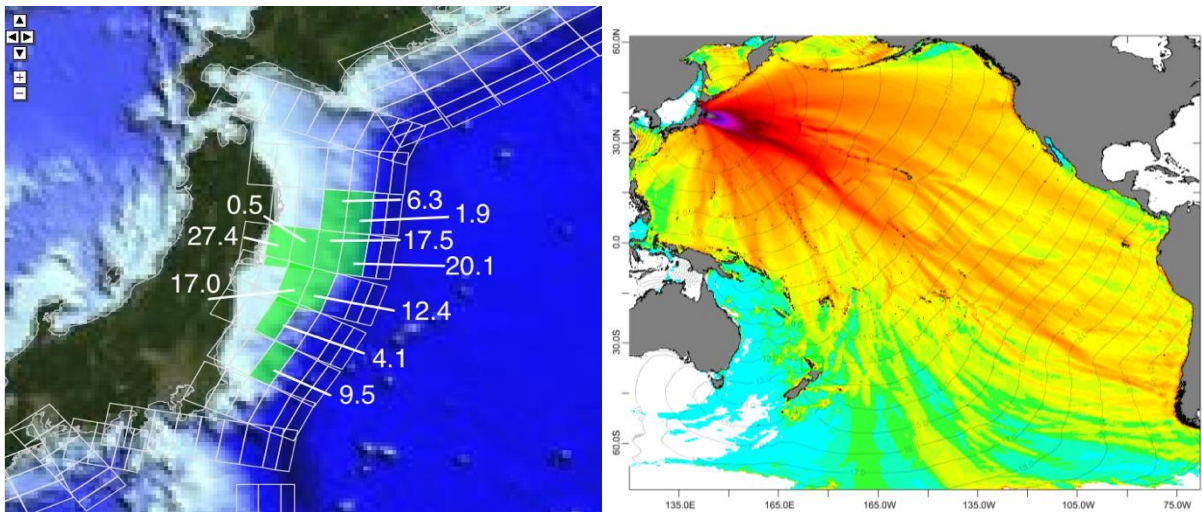


Figure 4.3 Tsunami source model (left) and the trans-Pacific propagation pattern (right) for the 2011 Tohoku, Japan tsunami. Slip amounts (in meters) for the individual fault segments are indicated in white.

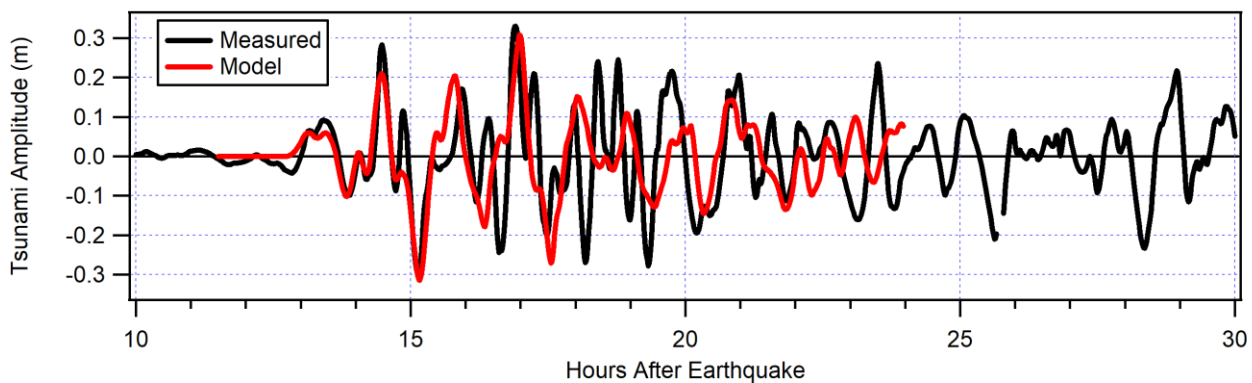


Figure 4.4 Modelled water level time series compared to measured data at Marsden Point for the 2011 Tohoku, Japan tsunami.

4.3 Case 3: The September 2nd, 2016 East Cape Earthquake and Tsunami

On 2nd September 2016 at 4:37 am NZST (1 September 16:37 UTC), a magnitude 7.1 (GeoNet) earthquake struck just north-east of the East Cape of New Zealand (Figure 3.10). The event was felt throughout the North Island. More than 4,000 people filed felt earthquake reports on the GeoNet community reporting system, with reports coming in from as far away as Chatham Island and Christchurch (GeoNet, 2017). The event created a small non-damaging tsunami that was recorded on tide gauges in Gisborne and across the Bay of Plenty.

This event is important in that it was relatively strong and occurred along the Tonga-Kermadec subduction zone, and in an area considered as the 'worst-case' source region for generating tsunamis affecting the East Cape, Bay of Plenty, Coromandel and Northland coasts – this due to its proximity and associated short travel times to these regions.

The source mechanism for this event was not, however, a straightforward subduction zone event. The strike of the fault plane was oblique, and the source region was displaced west of the trench axis, suggesting a seismic rupture within the overriding Australian plate (Figure 4.6, top panel). Additionally, the sense of the rupture was that of a 'normal' fault rather than a thrust or 'reverse' fault commonly associated with ruptures on a subduction zone interface. This means that the seafloor displacement above the source area was downward (i.e. negative) rather than upward (uplift). This is indicated by the direction of the slip vector arrows in the bottom panel of Figure 4.6.

To model this event using the pre-computed sources in the ComMIT database, some assumptions and approximations were necessary. Firstly, it was necessary to use a fault segment located to the east of the actual source region. Next, a negative average displacement was applied to the fault plane to produce a negative initial seafloor displacement. Two slip amounts were trialled, -0.4 m and -0.6 m.

The model results are compared to measured tide gauge data at Lottin Point and Tauranga Harbour in Figure 4.7. The comparison of the waveform at Lottin Point is remarkably good - given the approximations - with the results from the two source models neatly bracketing the measured data. Note that the modelled time series had to be shifted 7 minutes earlier to match the timing of the measured data. This accounts for the fact that the source region used in the model is located further away to the west of the actual source region, thus requiring more time for the wave to reach the tide gauge.

The results for Tauranga are not as good with the model over predicting the measured wave heights and requiring a 14-minute time shift to match the timing of the peaks and troughs. However, this is understandable given the very small size of the tsunami and the degree of attenuation that likely occurred as this small signal passed through the narrow entrance of Tauranga Harbour.

Given the limitations of the ComMIT model, the results are good and show that it can be used to accurately predict tsunami heights along the New Zealand coast from near-field tsunami sources.

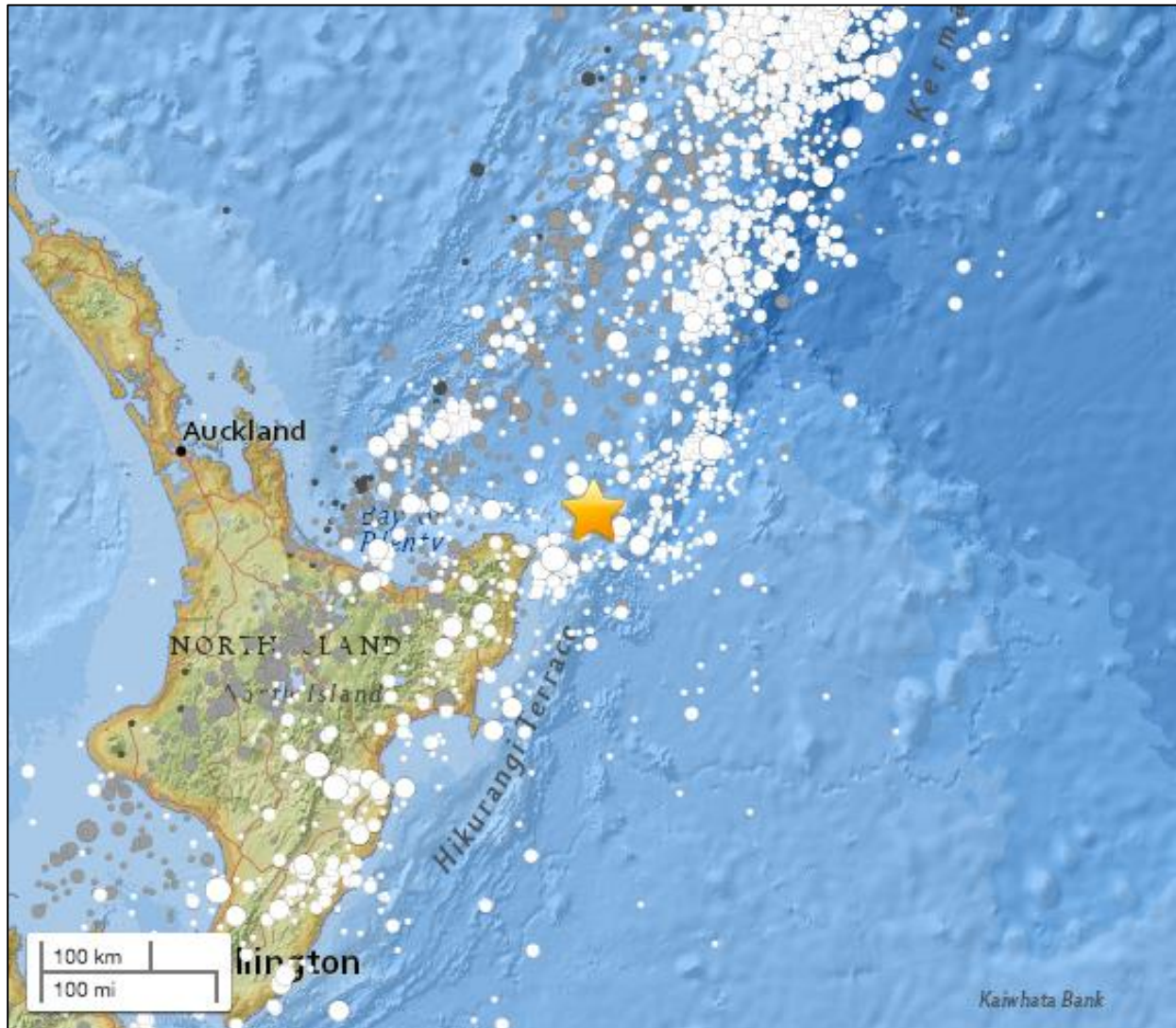
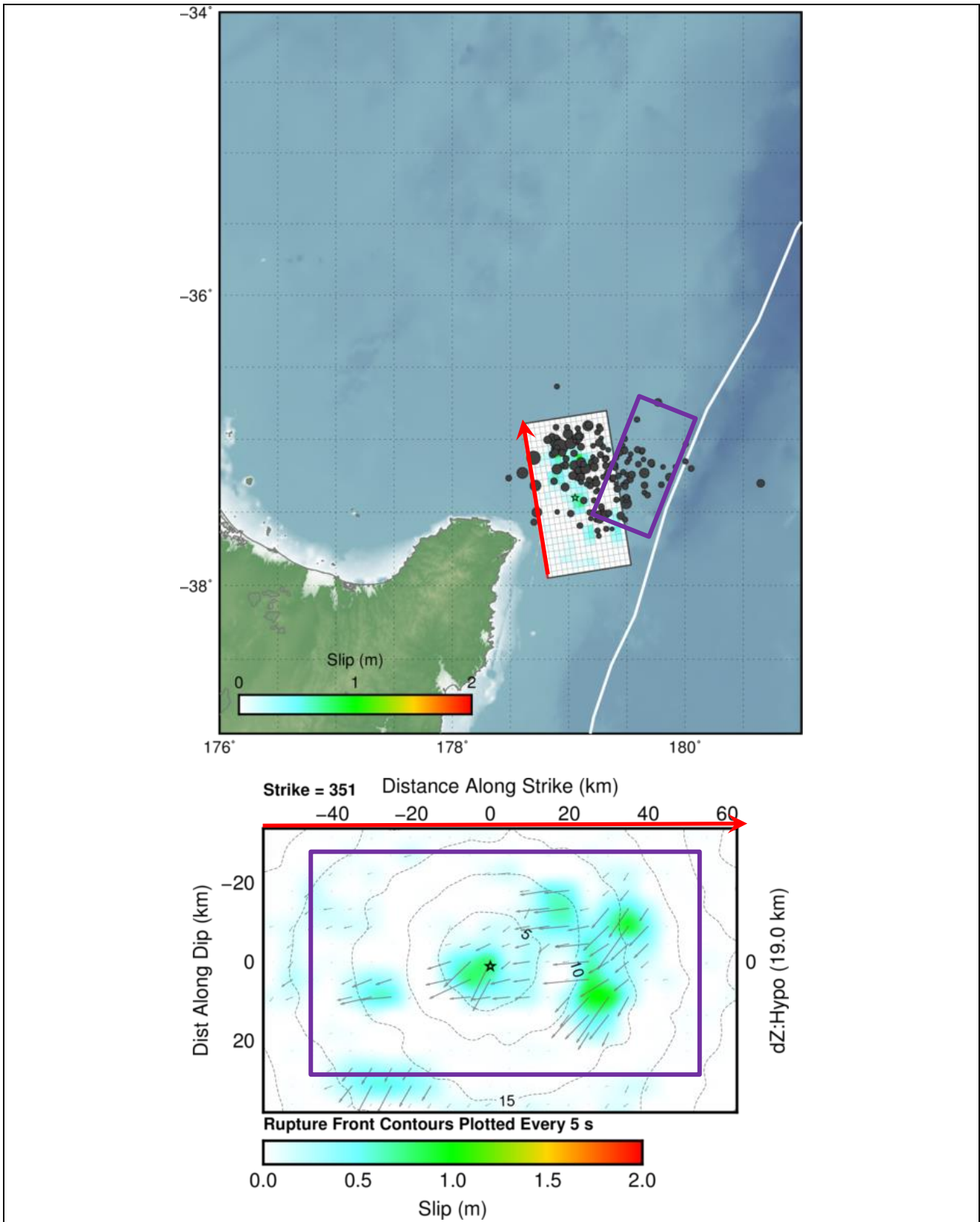


Figure 4.5 Source location of the September 2nd East Cape Earthquake (USGS, 2017).

Figure 4.6 (following page) Top panel: Earthquake source model for the September 2nd, 2016 East Cape earthquake (reproduced from USGS, 2016). The top panel shows the location of the fault plane (white region). Epicentre of the mains shock is indicated by a star with aftershocks indicated by black circles. Coloured patches indicate coseismic slip amounts according to the colour scale. The thin red line is the top of the fault plane. The white line is the axis of the Tonga-Kermadec Trench. The purple rectangle shows the location of a 100x50 km fault plane source available in the ComMIT tsunami modelling database. Bottom panel: A detail of the slip distribution along the fault plane with the amount of slip indicated by the colour scale. The location of the earthquake hypocentre is indicated by the star with the arrows indicating the direction of the rupture displacement. The contour lines are the timing (in seconds) of the rupture. The red arrow at the top of the fault plane corresponds to the red arrow in the upper panel. The purple box shows the dimensions of a 100x50 km fault plane.



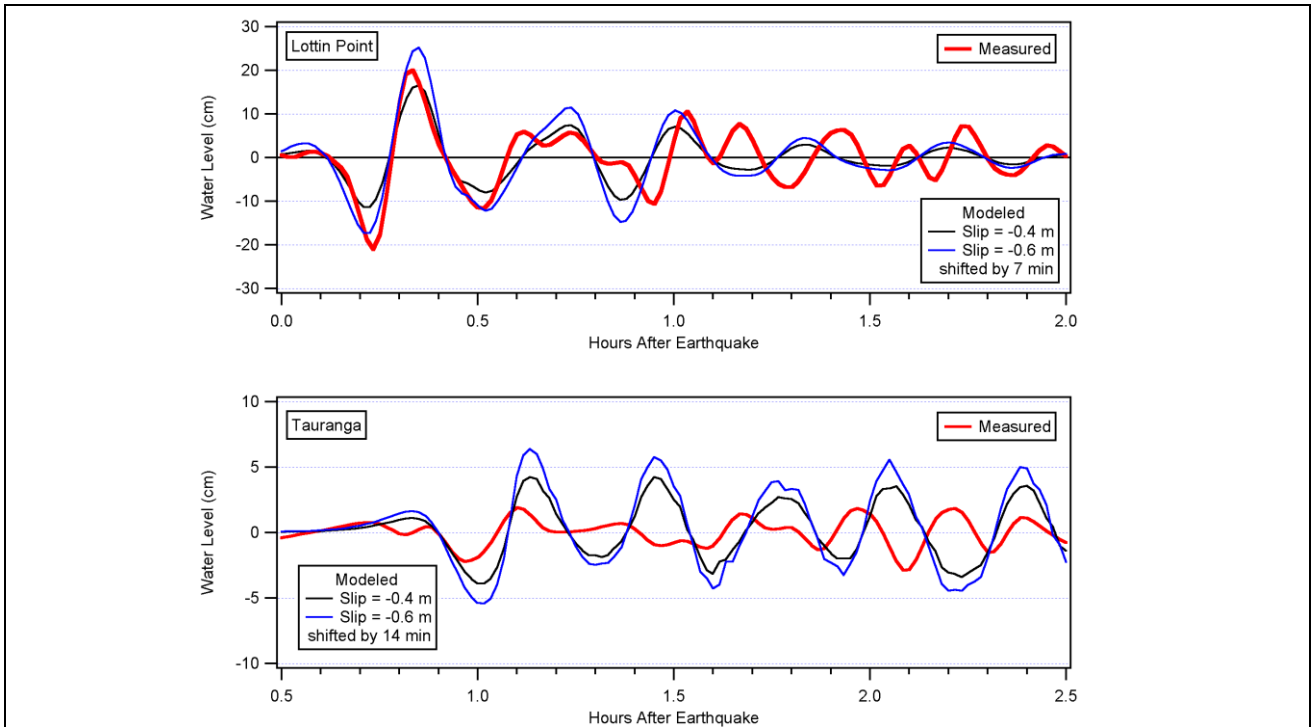


Figure 4.7 Modelled (blue and black traces) versus measured (red trace) water levels at Lottin Point (top) and Tauranga (bottom) for the 2nd September 2016 tsunami.

4.4 Modelling The 1976 Event in Tutukaka

Early in the morning of January 15, 1976 two relatively large earthquakes occurred within one hour of each other along the Tonga-Kermadec Subduction Zone, approximately 1100 km north east of New Zealand's East Cape (Todd and Lay, 2012). The first shock occurred at 4:56 AM NZDT with the second coming at 5:47 AM. The event generated a small tsunami which was recorded through the Pacific Ocean including several sites in New Zealand with noticeably stronger effects in Tutukaka Harbour where the tsunami reached heights of 0.2-0.75 m (newspaper reports are inconsistent) and caused damage to several boats and some port structures such as piles and marker buoys (Downes *et al.*, 2017).

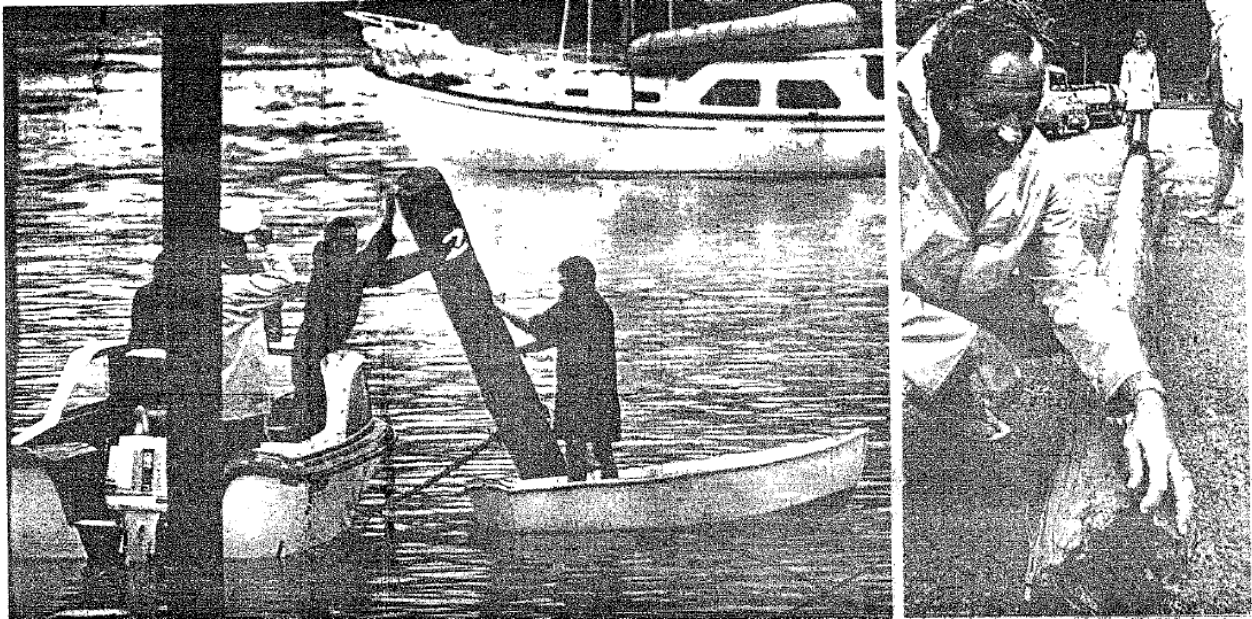


Figure 4.8 Photos from a newspaper account of the 1976 tsunami in Tutukaka. The caption reads “[Left]: A yacht heads out to sea at Tutukaka to escape the tidal wave. In the foreground men steady a pile loosened by surging water. [Right]: Mr D. Cutfield, owner of the launch Willie O inspects a pile snapped off at the base.

Reports suggest that the second earthquake was slightly larger and shallower than the first event and was likely the source for the subsequent tsunami. Among the accounts reported by Downes *et al.* (2017) are descriptions of yacht being torn from their moorings, a surge of 0.75 m, ‘a great big whirlpool’ and current speeds estimated at 8 knots.

To model the event we used a source model 100 km long by 50 km wide with a uniform slip of 2.8 m occurring along the deeper segments of the TK Trench as indicated in Figure 4.9. The resulting model output is presented in Figure 4.10 and Figure 4.11 and agree well with the eyewitness reports. Our model predicts a maximum tsunami height of 0.81 m while eyewitnesses at the time reported a height of 0.75 m. Additionally the timing of the modelled maximum surge compares well with eyewitness accounts that the strongest effects occurred around 8:45 am on January 15th. In terms of current speeds, the model suggests currents of up to 10 knots, strongest in the entrance to the inner harbour area, while reports from the time estimated current speeds at 8 knots.

Overall, it seems that the modelling is consistent with the available observational data and provides further confidence in the veracity of the modelling methodology used here.

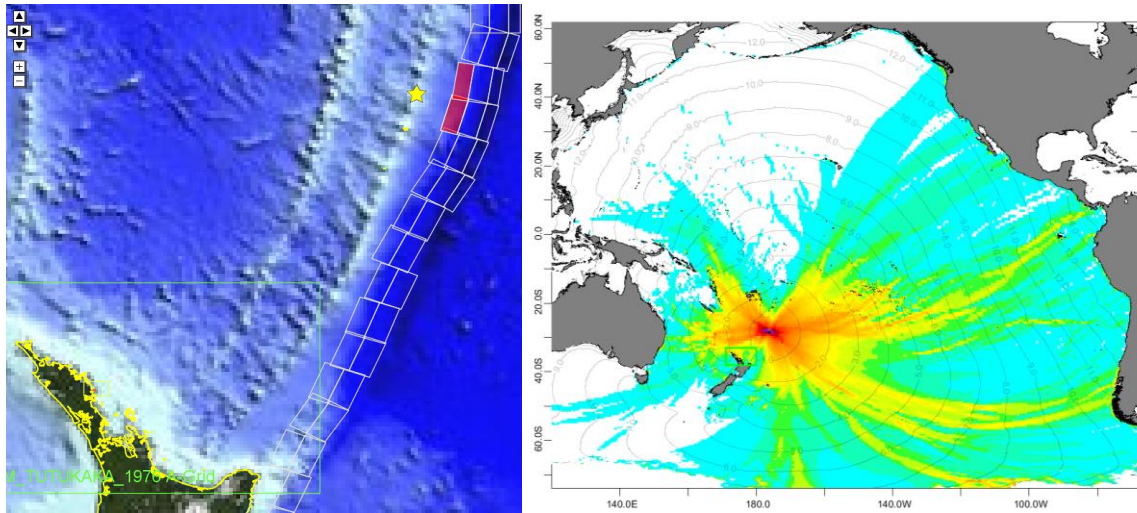


Figure 4.9 The source segments (left) and the trans-Pacific propagation pattern.

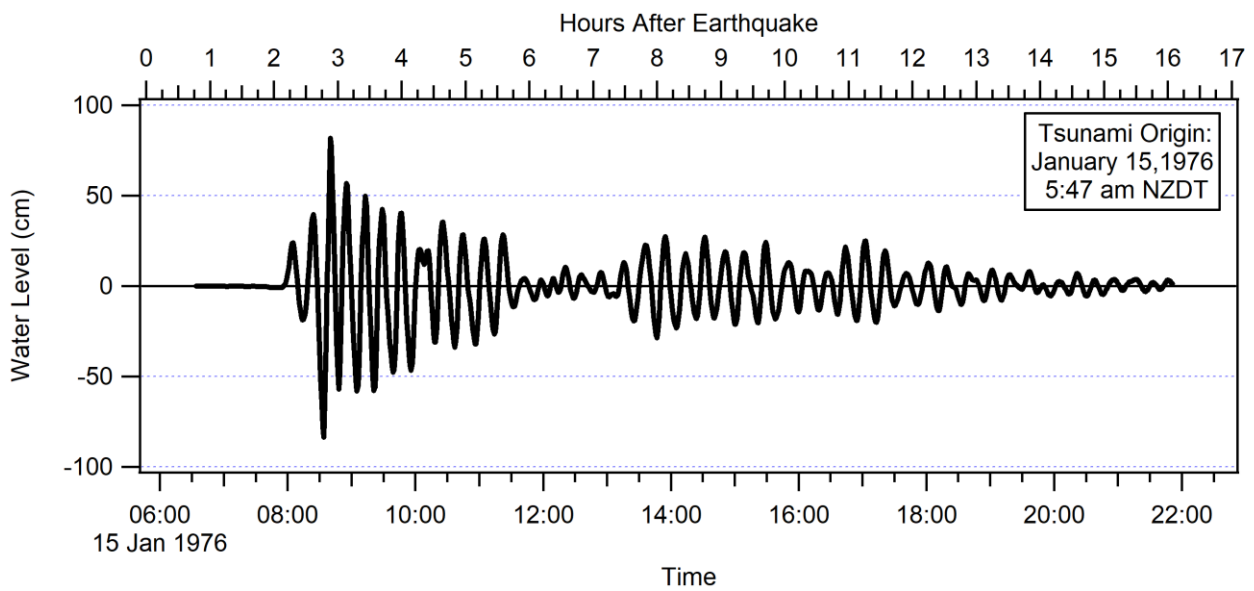


Figure 4.10 Time series of modelled tsunami water level inside Tutukaka Harbour.

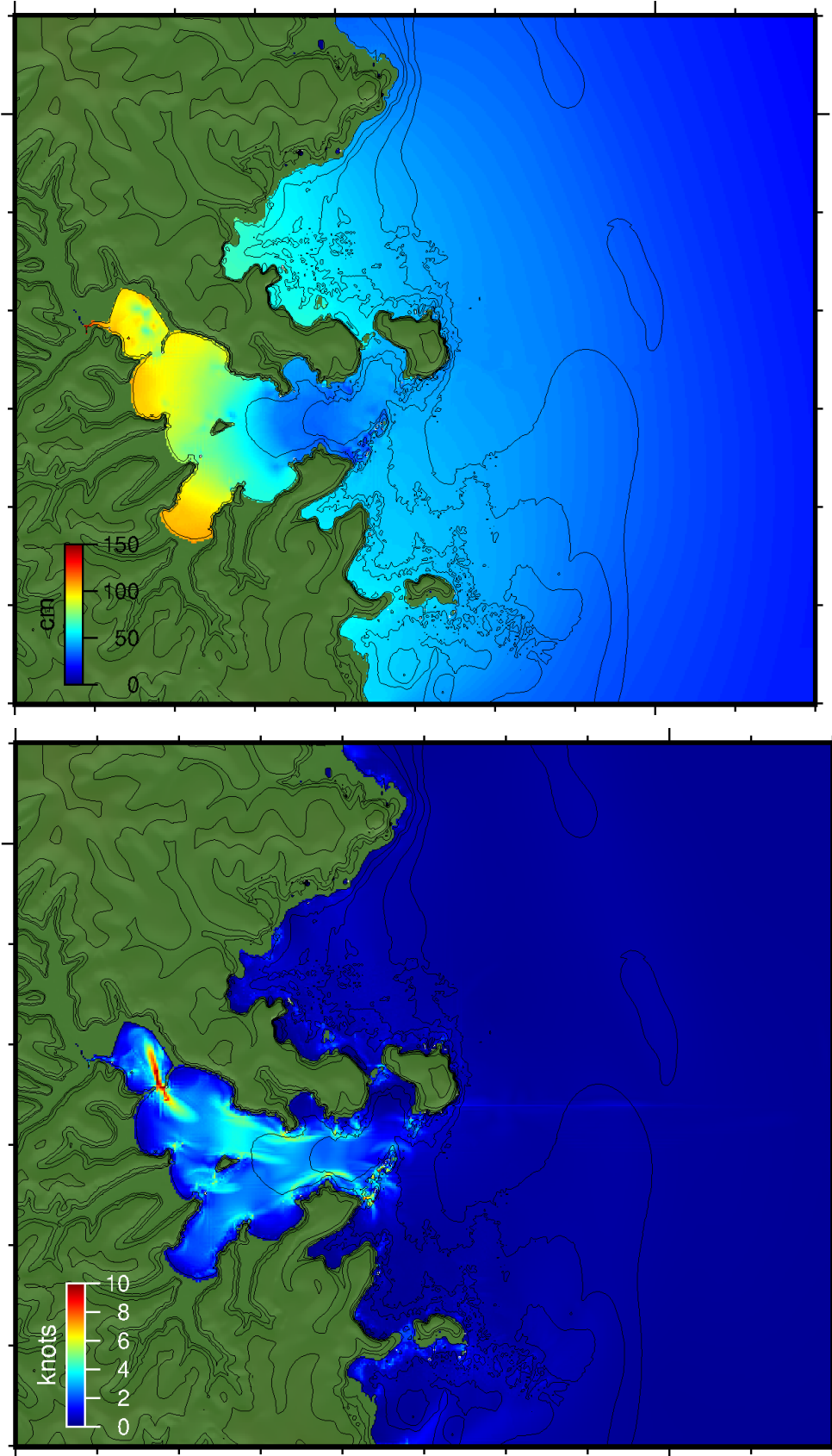


Figure 4.11 Modelled Maximum tsunami amplitude (top) and current speed (bottom).

4.4.1 1976 Source Sensitivity Assessment

Because the details of the 1976 source mechanism are not well defined, we undertook a sensitivity analysis of the tsunami wave forms produced by ComMIT at Tutukaka for a range of different tsunami sources that could be responsible for the 1976 event. To this end we used a 2x2 patch of source segments and varied the distribution of the slip over 13 possible combinations while maintaining a constant earthquake magnitude. This included putting all the slip on each of the four segments, distributing the slip evenly over two segments (either two shallow, two deep or a deep to shallow rupture) as well as spread evenly over the four segments. We also trialled cases where the slip was partitioned nonuniformly between the deep and shallow fault segments. These combinations are laid out in Figure 4.12.

The model results are presented in Figure 4.13 and show that the predicted tsunami heights at Tutukaka are relatively insensitive to the details of the initial condition, particularly in the first 3-4 hours of tsunami activity. However, we note that Source 5 (the source used in the initial assessment described above and shown in black in Figure 4.13) is somewhat smaller than the other cases from 5.5 to 7.5 hours after the earthquake before falling back in with the rest of the simulations after that.

The point of this exercise was to show that Tutukaka Harbour is vulnerable to tsunami generated by relatively small earthquakes located along the Tonga Kermadec Trench. However, based on the output from this sensitivity study, we would be able to generate precomputed predictions of the potential tsunami effects for several different sources that can be used to give guidance for appropriate action within the time between the earthquake and the expected tsunami arrival. Although these detailed, Tutukaka-specific scenarios are out of the scope of this project they should be part of an additional study considering the effect of local or regional earthquakes on maritime facilities.

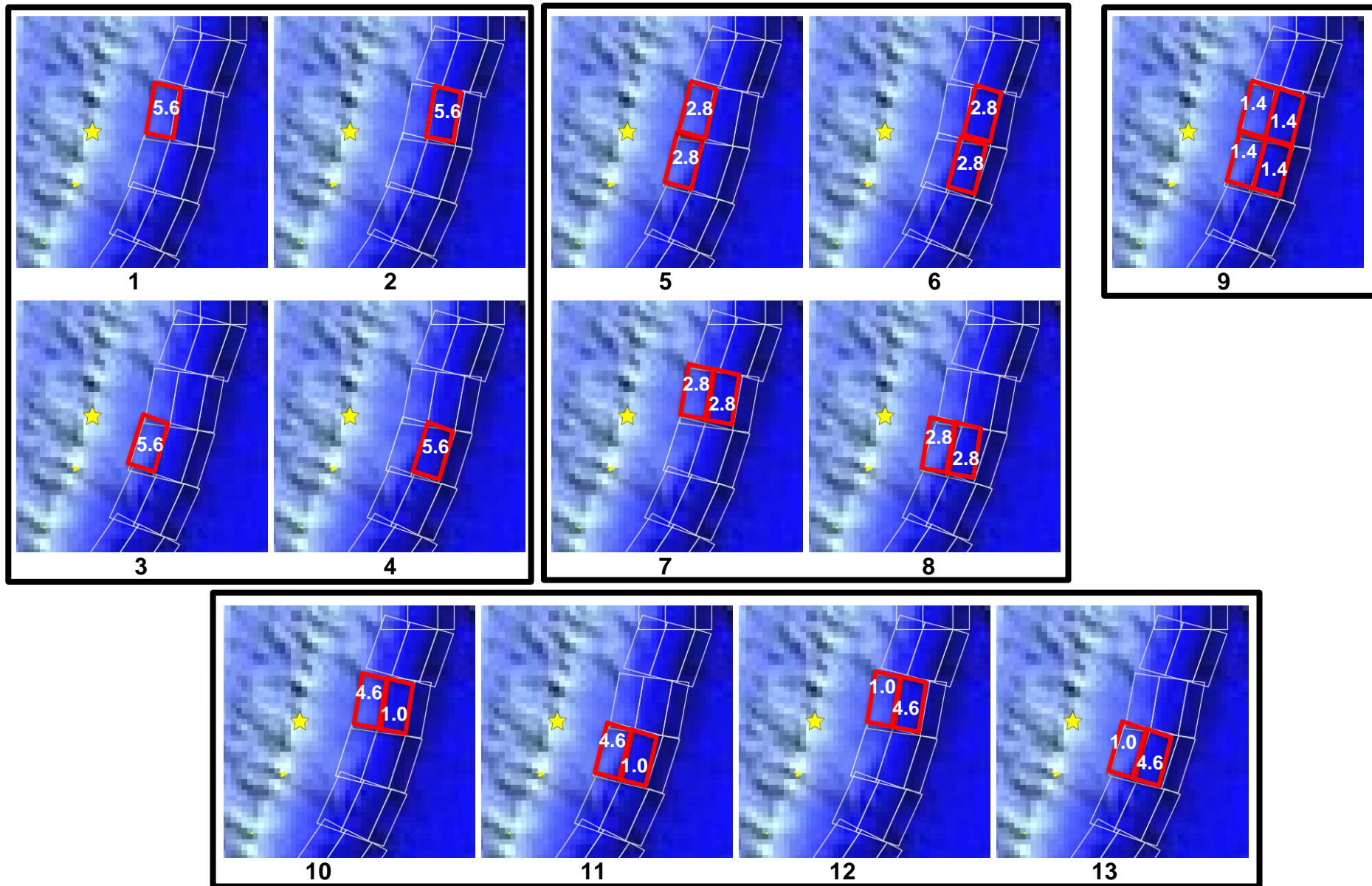


Figure 4.12 Source segments and slip amounts for the January 1976 Kermadec earthquake and tsunami.

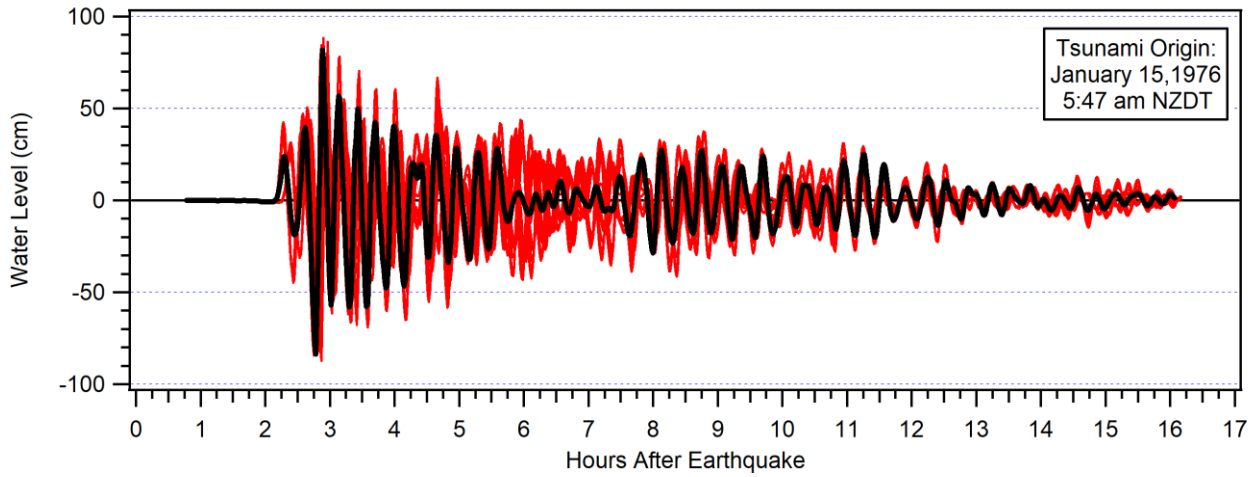


Figure 4.13 Comparison of modelled time series outputs at Tutukaka for the 13 different source scenarios. The black line is Source 5, the one used in the initial modelling shown in Figure 4.9 through Figure 4.11

5 FAR-FIELD SENSITIVITY ANALYSIS

The relative effect of each tsunami source can be assessed through a sensitivity analysis whereby we determine which source is responsible for the strongest tsunami effects at a particular location, this is illustrated in Figure 5.2 and Figure 5.3 for northern New Zealand and the Bay of Islands regions and in Figure 5.4 for Tutukaka. To accomplish this, we split the model runs in to the 6 regional groups as per Figure 5.1 below. For each figure, the colour bar represents the source number that produced the largest tsunami amplitude (or current speed in the fine scale grids) at that location in the model grid.

In the large-scale outer grid (Figure 5.2), most sets show a complex pattern of sources contributing to the maxima. The exceptions are Set 2 where Source 19 is clearly dominant and Set 6 where source 70 is dominant. A somewhat similar pattern is seen in the regional scale grids around the Bay of Islands (Figure 5.3). Zooming in to the detailed grid for Tutukaka (Figure 5.4), one or two sources from each set can be seen to dominate the tsunami height plots, however, in the current speed plots the pattern is not as clear. We also see some interesting effects such as in Set 3 where sources 33 and 34 switch between dominance for tsunami height and current speed inside and outside of Tutukaka Harbour. This variability underlies one of the basic assumptions of this project which is that tsunami heights do not necessarily correspond to stronger tsunami currents. In Table 5.1 we list which sources generally produce the highest tsunami heights within each fine scale modelling region. This is not a rigorous quantitative accounting, but rather a qualitative assessment based on visual inspection of each plot. We did not do this with the current speed plots because of the complexity of the patterns which did not indicate a clear dominant source for any other than Set 6.

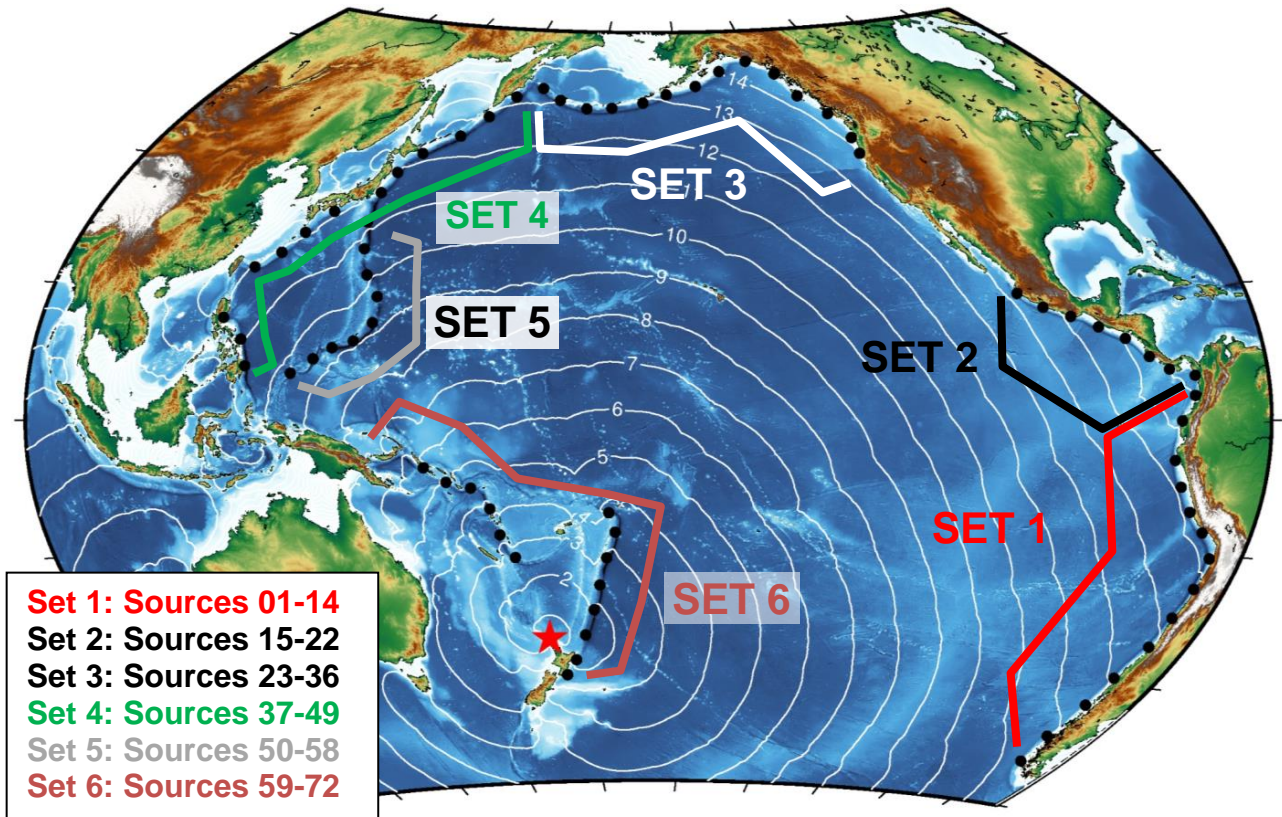
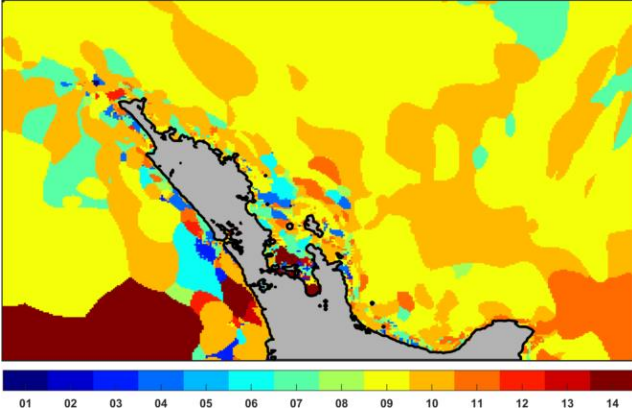


Figure 5.1 Tsunami source regions. Black dots denote the centre of each individual tsunami source.

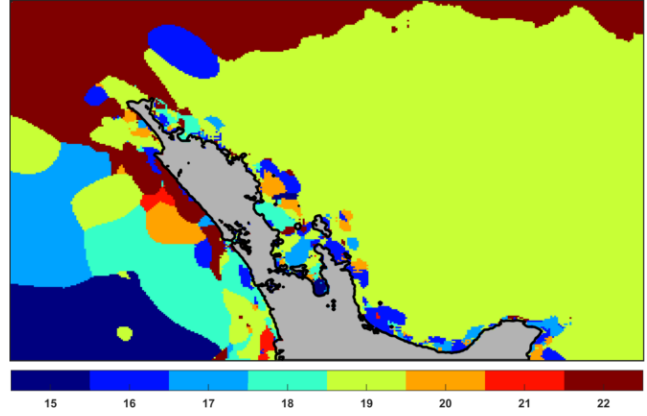
Table 5.1 Source numbers contributing to the maximum tsunami amplitudes observed at each region.

	Set 1	Set 2	Set 3	Set 4	Set 5	Set 6
Doves Bay	10	18	33,34,35	48	57	70
Marsden Point	9	16,18	24	40,48	51,56,57	70
Opuā	6	16,20	35	40	57	70
Tutukaka	19	20,22	33,34	40,42	50	70
Waitangi	6,9	16,20	28	40	57	70
Whangaroa	10	16,19	35	48,42	57	70
Whangaroa Entrance	9,10	16	34,35	39,40	54,55	70

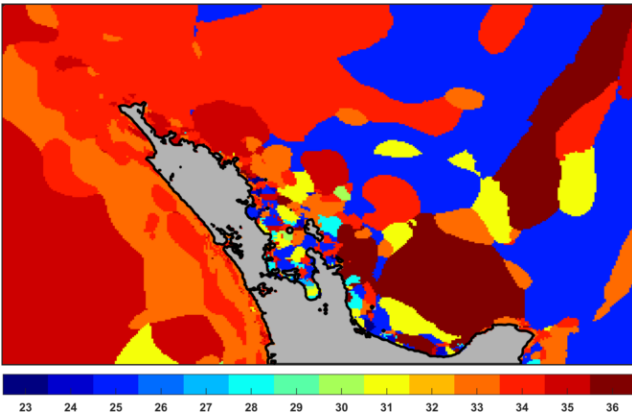
Set 1



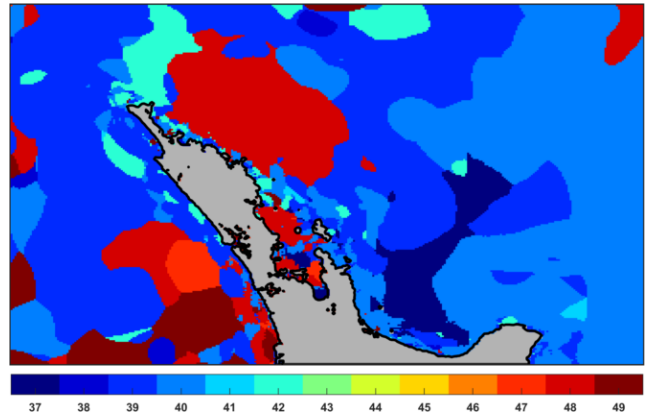
Set 2



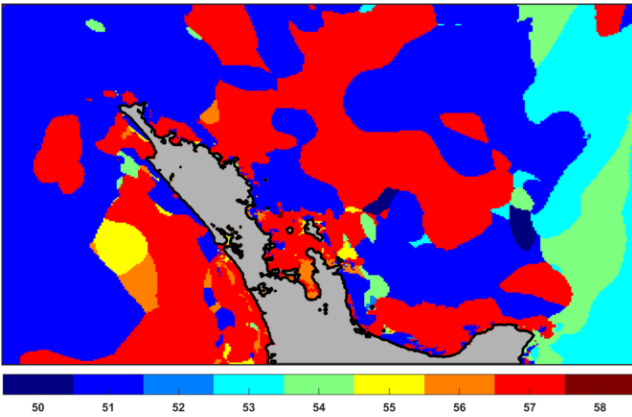
Set 3



Set 4



Set 5



Set 6

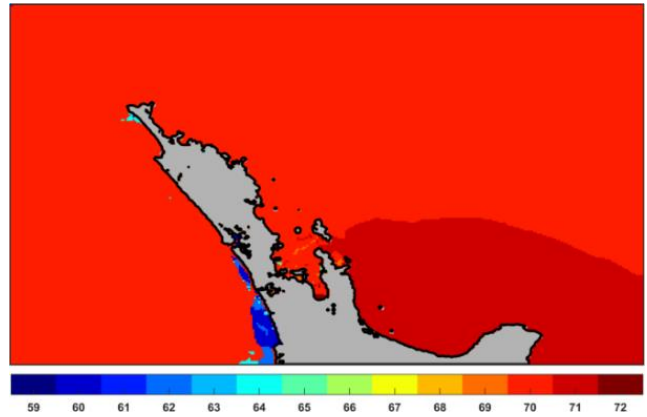
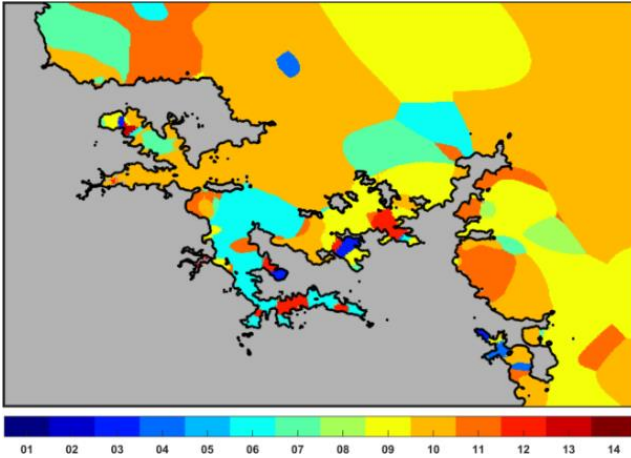
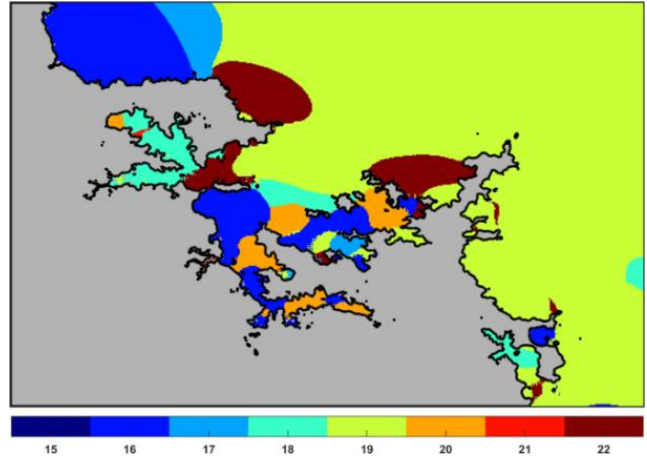


Figure 5.2 Maximum height by source around northern New Zealand.

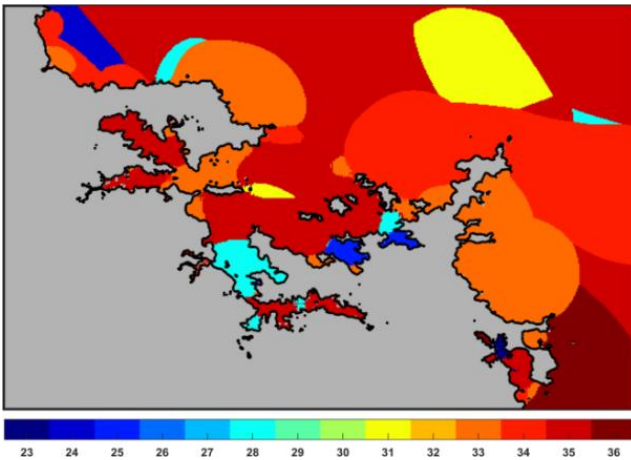
Set 1



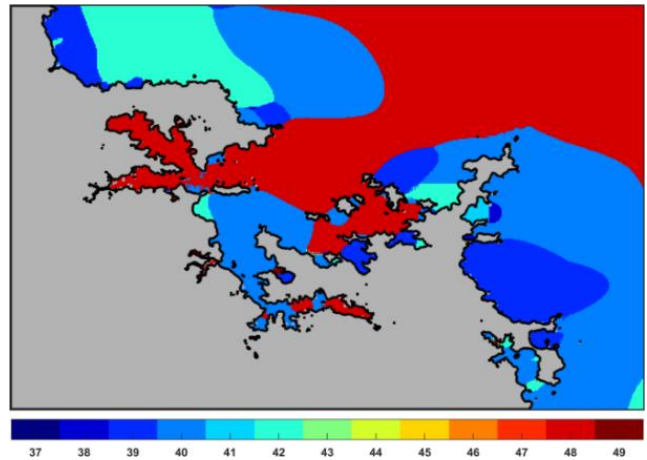
Set 2



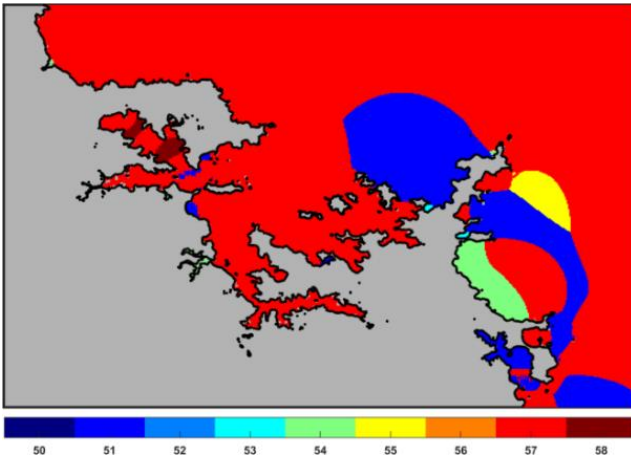
Set 3



Set 4



Set 5



Set 6

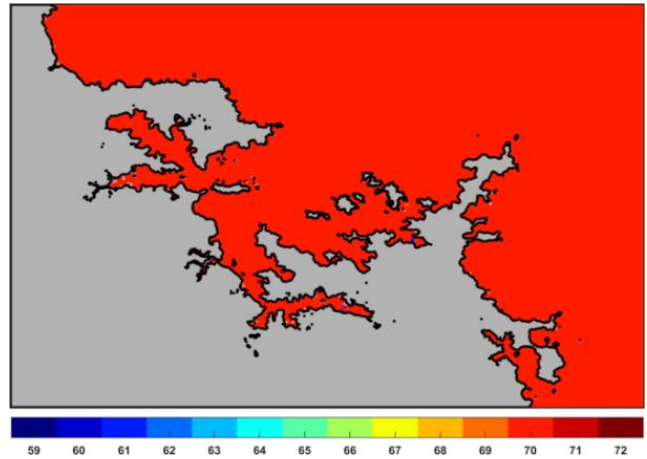
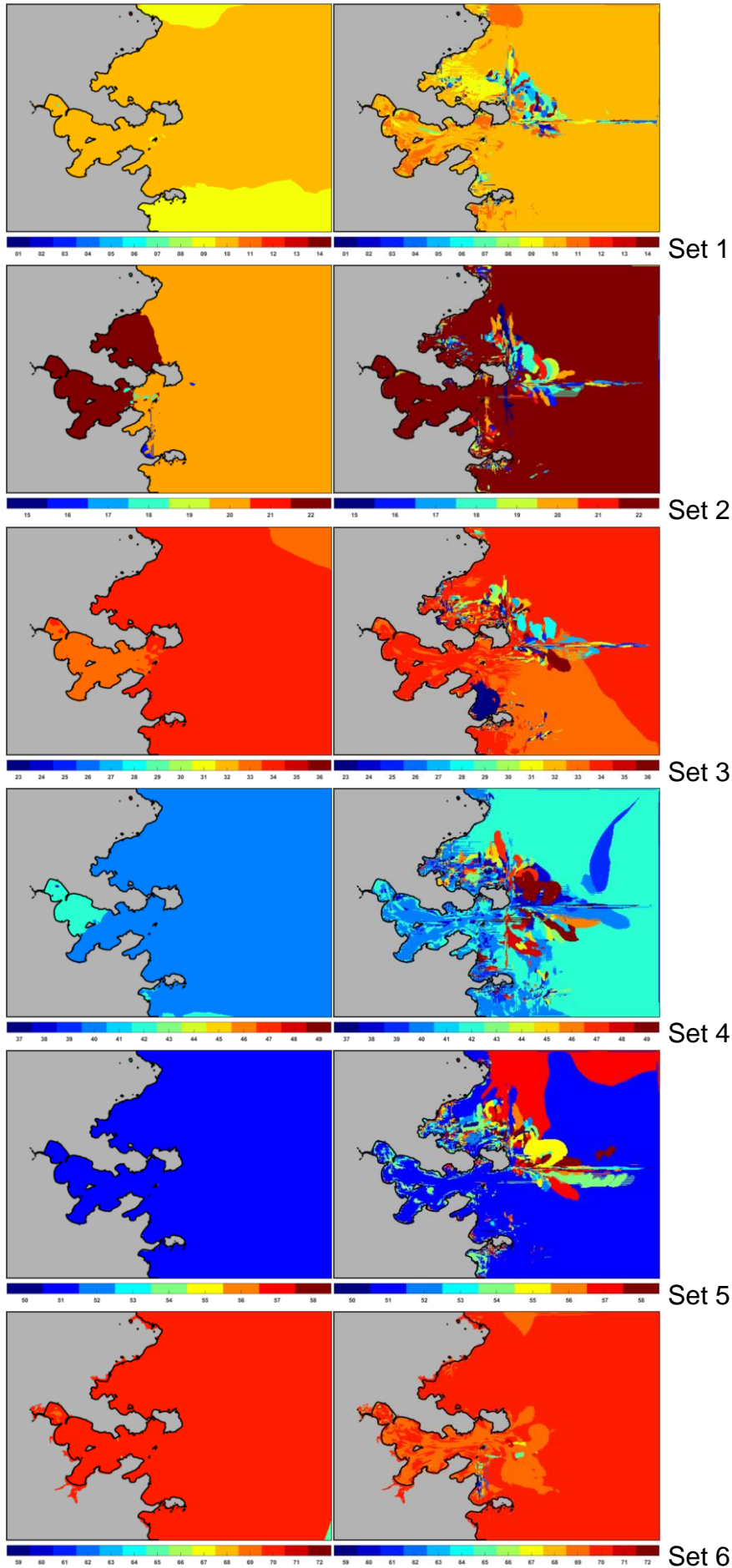


Figure 5.3 Maximum height by source for the Bay of Islands area.

Figure 5.4 (next page) Maximum height by source (left column) and maximum current speed by source (right column) for Tutukaka.



6 DEVELOPMENT OF MARITIME GUIDANCE PLAYBOOKS

The 'playbook' concept developed and presented here is an extension and continuation of several projects. In New Zealand, as noted in Section 1.1.2, Power and Gale (2010), developed a system for rapidly assessing New Zealand-wide tsunami threat levels based on precomputed numerical modelling scenarios of large magnitude earthquakes around the Pacific Rim. In California, the 2010 Chile and 2011 Japan events prompted state officials there to begin the development of scenario-based threat assessment products (Wilson and Miller, 2012). These efforts were expanded in the work of Lynett *et al.* (2012, 2014) and ran concurrently with further developments in New Zealand where the first generation of port-specific threat assessment tools were being developed as described in Borrero *et al.* (2014).

While scenario-based threat assessments provide a rapid means of evaluating a tsunami's potential impact, they do have their drawbacks as noted in Power and Gale (2010) who wrote:

“One drawback of pre-calculated model scenarios is that any actual event is unlikely to precisely match any one scenario. The location will in general not correspond exactly to one of the scenarios, and in most cases the magnitude will have to be rounded up to the nearest modelled magnitude, or the model results subject to empirical scaling. Even with a close match to location and magnitude there are other factors, such as the earthquake depth and detailed slip-distribution, that affect the scale of the tsunami generated.”

Thus, it is important to use these products as guidelines and not as absolute indicators of a tsunami impact.

6.1 Individual Products Derived from Model Output

As noted above, 72 earthquake sources were considered at three magnitudes with the tsunami effects modelled in detail for seven sites. This yields a total of (72 x 3 x 7 = 1265) separate simulations. For each simulation, the following plots have been prepared and are included in the final guidance playbook. Each component is described in detail below using the Magnitude 9.0 source Number 10 scenario as modelled in Tutukaka.

Maximum tsunami height plots: Plots of the maximum modelled tsunami amplitude at different grid scales are an important part of the overall hazard assessment. For this we first include a global propagation plot that shows the radiation of the overall tsunami energy across the Pacific and a zoom in of this data around New Zealand (Figure 6.1). Note however that this is presented with a logarithmic colour scale which allows for a better display of the spread of tsunami energy across the Pacific.

We then switch to a narrower colour palate for the displaying the maximum modelled tsunami amplitude at a regional scale and in the detailed area of interest (Figure 6.2). In these plots we have opted to make them as simple as possible using a grey fill for land areas and a thick black line to indicate the shoreline. In the regional grid, the location of the high-resolution local grid is indicated with a red rectangle. Areas of on land inundation are indicated where the colour from the wet areas spill over the shoreline on to the land. Note that the latitude and longitude tick marks are intentionally removed from these plots as it is assumed that the users of these maps would be sufficiently aware of the layout of their local area and the relative locations of things. The amplitudes of these plots are expressed in meters above mean sea level.

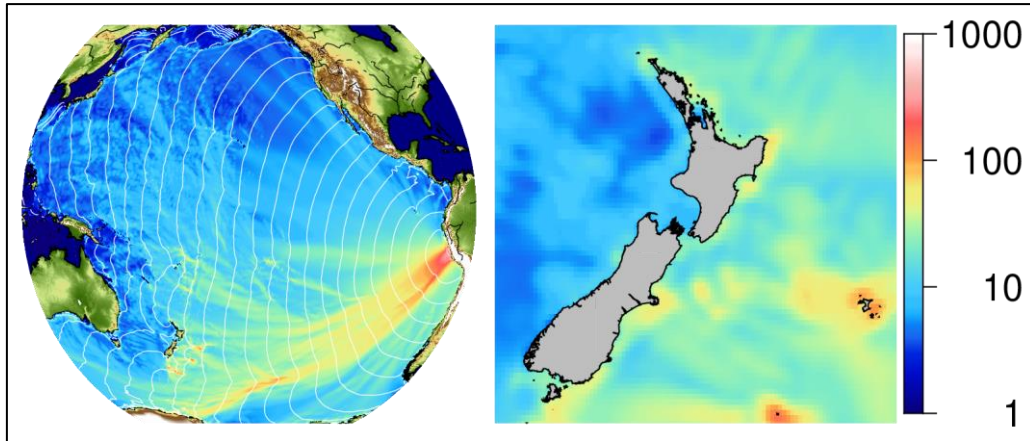


Figure 6.1 Trans-Pacific propagation. Tsunami height in cm.

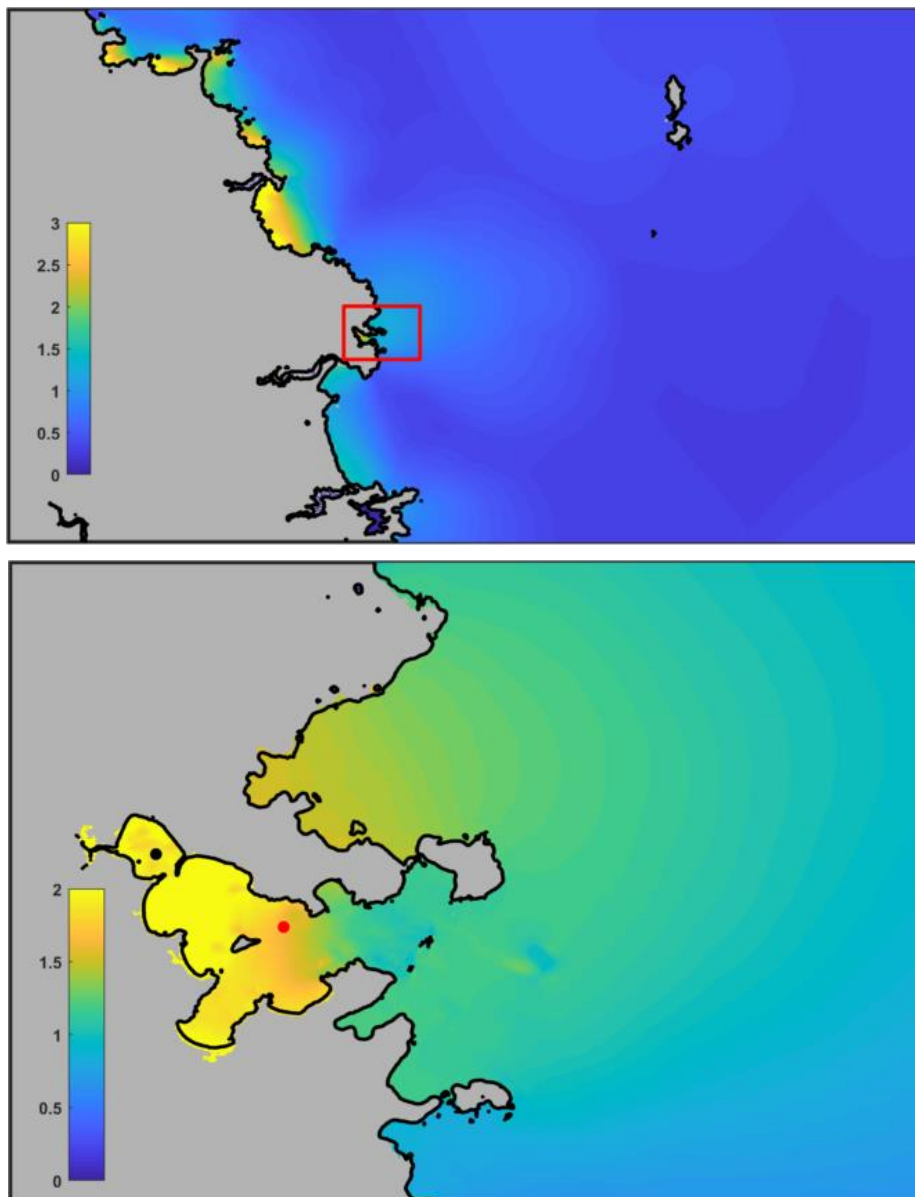


Figure 6.2 Maximum tsunami amplitudes in the regional and high-resolution local grids (Tutukaka, Source 10, Magnitude 9.0).

Tsunami Timeseries Plots: For each scenario we plot a time series of tsunami water level at two locations inside the high-resolution model region (Figure 6.3). The trace of the timeseries plot is colour coded to a marker dot in the high-resolution maximum tsunami amplitude plot. The maximum and minimum tsunami heights are indicated on each plot as well as the modelled arrival time for the first tsunami wave.

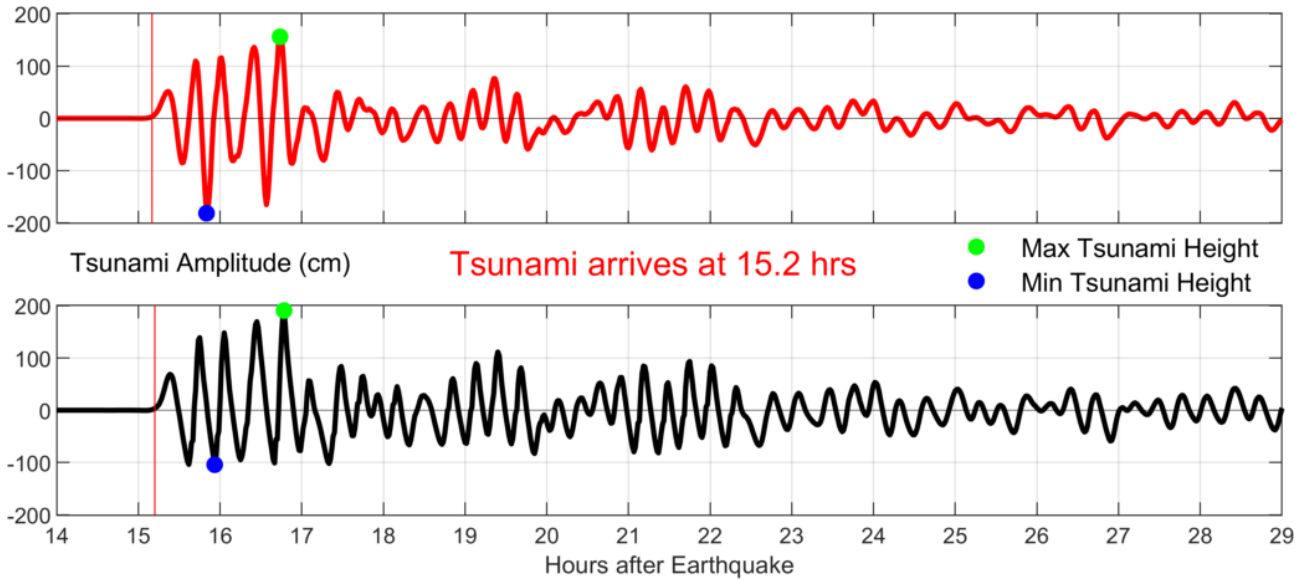


Figure 6.3 Time series at 2 locations in C grid, height expressed in cm.

Maximum Current Speed Plots: These are plots of maximum computed tsunami induced currents in the high-resolution model grid. The data is plotted in knots using a discrete colour palette for quick/easy identification of zones prone to high or low current speeds for that source (Figure 6.4).

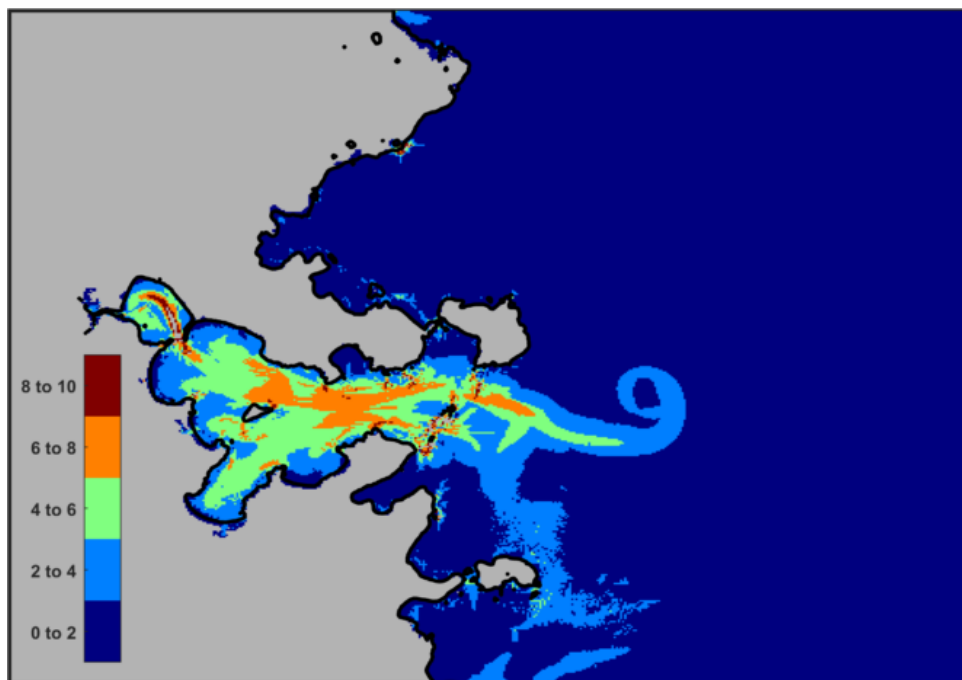


Figure 6.4 Maximum tsunami induced currents (knots) in discrete colour palette.

Tsunami Current Speed ‘Time Over Threshold Plots’: These plots show the duration that current speeds are predicted to be over a certain threshold speed (i.e. 3 knots). Hence the colour scale is in HOURS after tsunami arrival into the model domain (Figure 6.5).

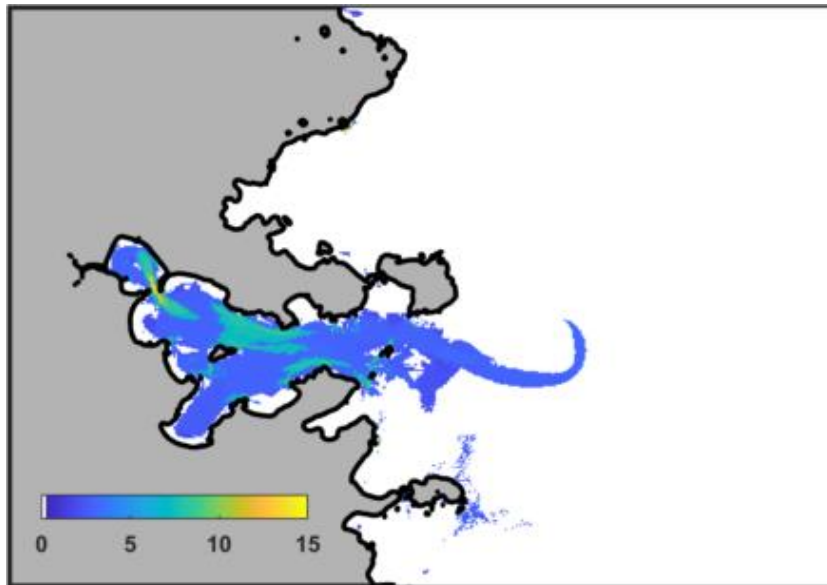


Figure 6.5 Tsunami current speed duration over threshold plot.

Tsunami Current Speed vs. Depth Scatter Plot: This plot shows all the modelled maximum current speeds plotted against the depth at that particular grid node location. The resulting plot can be used to determine an advisory depth for vessel evacuation in order to stay out of currents of a certain speed (Figure 6.6). For these plots we have chosen to highlight a speed of 3 knots in order to determine a safe evacuation depth. For the scenario shown below, a vessel would have to move to a depth greater than approximately 35 m in order to stay away from currents exceeding 3 knots.

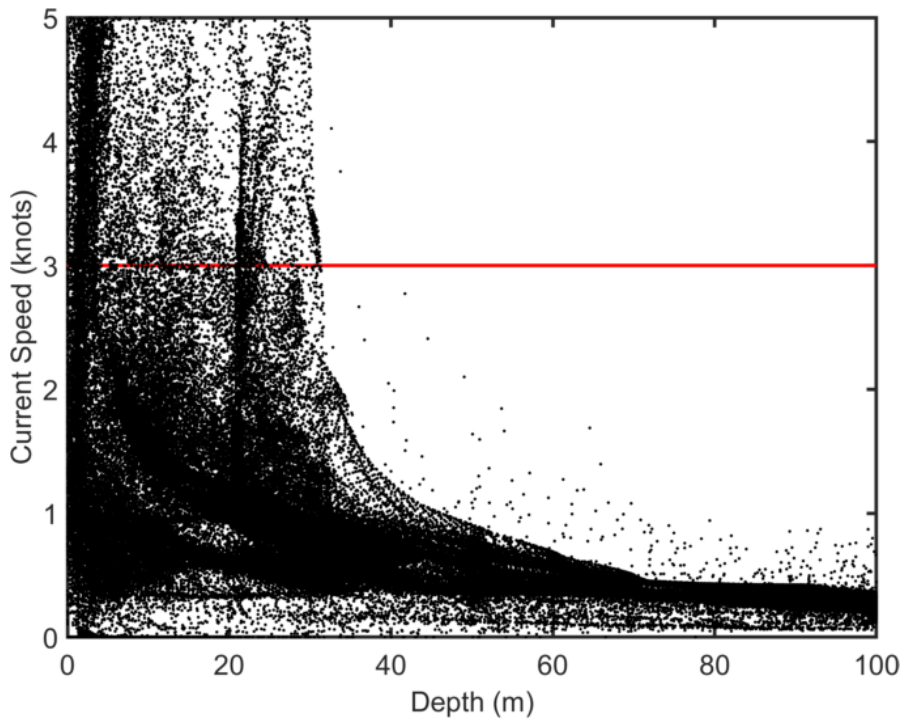
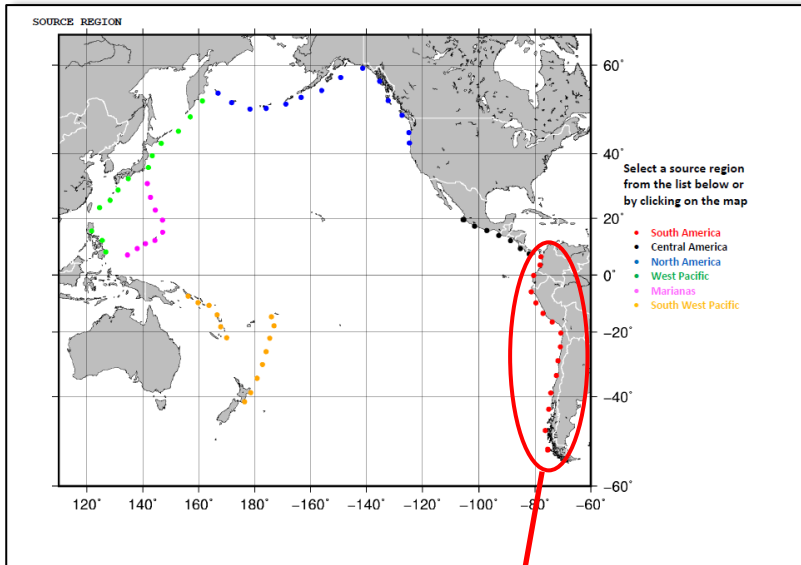


Figure 6.6 Tsunami current speed vs. depth scatter plot.

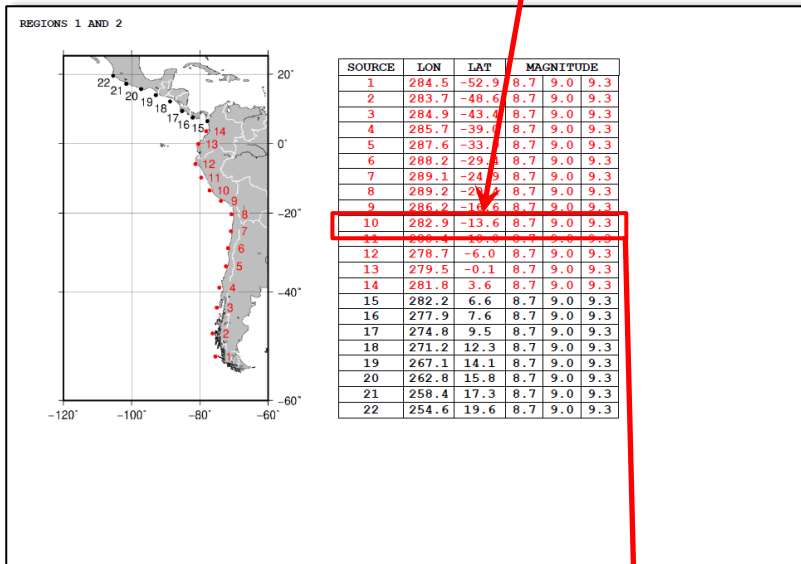
6.2 Sample Playbook Pages

The individual plots described above are then assembled into individual pages, one for each source over the three magnitudes for a total of 216 sheets. These are then assembled into seven separate (one for each site) interactive or 'clickable' PDF documents which a user can navigate by clicking with their mouse. A sample of the workflow for getting to the page of interest is shown in Figure 6.7.

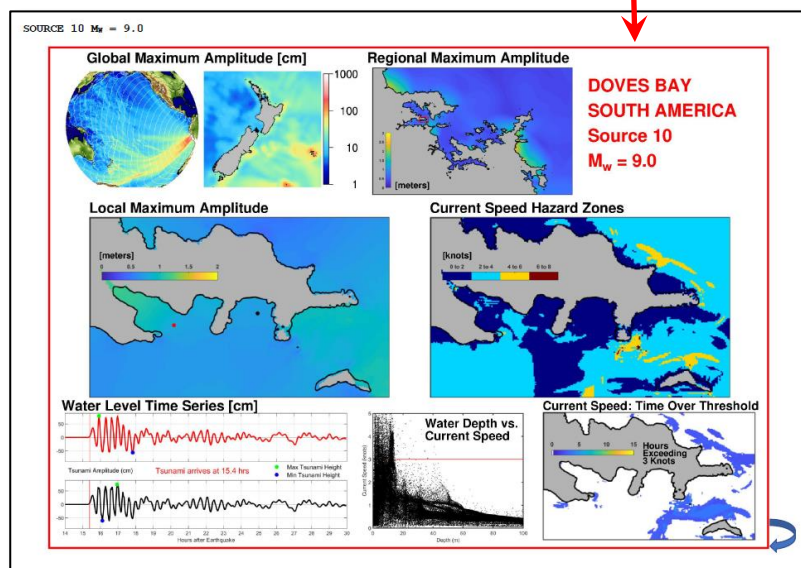
In addition to the selection and map pages, each playbook has a two-page worksheet that is designed to be printed by the user during an event. By going through the work sheet, the user will be directed on how to correctly determine critical information such as the event magnitude, location as well as the first arrival times and the timing of the occurrence of maximum and minimum tsunami heights.



1) Select the source region either by clicking the map or from the list.



2) Select the source with the appropriate magnitude and location



3) You are taken to the appropriate playbook page. You can return to the region selection map by clicking on the return arrow in the lower right corner of the page.

Figure 6.7 Sample of the navigation flow through the playbook pages.

**DOVES BAY MARINA
TSUNAMI EVENT
MARITIME RESPONSE WORKSHEET**

I) EVENT AND RESPONDER INFORMATION

RESPONDER NAME _____

POSITION _____ DATE/TIME _____

EVENT NAME _____

II) EVENT ORIGIN TIME

UTC _____ : _____ AM/PM
 HH MM

LOCAL _____ : _____ AM/PM
 HH MM

III) SOURCE LOCATION AND SIZE

COUNTRY/REGION/OCEAN _____

LONG (E/W) LAT (N/S) _____

EARTHQUAKE MAGNITUDE _____

IV) REFER TO INTERACTIVE PDF

1) SELECT MAGNITUDE
2) SELECT REGION
3) SELECT SOURCE (NEAREST LONG/LAT)

4) OPEN SCENARIO EVENT PAGE

NOTE SCENARIO EVENT CODE HERE

5) PRINT SCENARIO EVENT PAGE IF POSSIBLE

VI) DETERMINE TSUNAMI ARRIVAL TIME

1) GO TO TRAVEL TIME (TT) CHART
2) LOCATE SOURCE ON TRAVEL TIME CHART
3) COUNT COPTOUR LINES TO SOURCE LOCATION
4) THIS IS THENUMBER OF HOURS UNTIL THE FIRST ARRIVAL OF TSUNAMI.

HOURS UNTIL FIRST ARRIVAL

ADD HOURS UNTIL FIRST ARRIVAL TO ORIGIN TIME (LOCAL) TO GET LOCAL ARRIVAL TIME. NOTE BELOW

<input type="text"/>	<input type="text"/>	<input type="text"/>
HH	MM	AM/PM

THIS IS THE LOCAL ARRIVAL TIME

NB: THIS IS FOR GUIDANCE ONLY. TSUNAMI EFFECTS CAN PERSIST FOR MANY HOURS OR DAYS AFTER FIRST ARRIVAL. STRONGEST TSUNAMI EFFECTS ARE GENERALLY OBSERVED SEVERAL HOURS AFTER FIRST ARRIVAL.

VII) REFER TO SCENARIO EVENT PAGE DATA PLOTS (PRINTED OR ONSCREEN). TAKE NOTE OF:

1) MAXIMUM PREDICTED TSUNAMI AMPLITUDE IN YOUR REGION _____ CM

2) MAXIMUM PREDICTED TSUNAMI CURRENT SPEED IN YOUR REGION _____ KNOTS

3) ZONES OF PREDICTED STRONG CURRENTS _____

4) TIMING OF PREDICTED MAXIMUM AND MINIMUM TSUNAMI HEIGHTS.

LOCATION 1 MAX:
MAX _____ CM AT _____ HRS
MIN _____ CM AT _____ HRS

LOCATION 2 MAX:
MAX _____ CM AT _____ HRS
MIN _____ CM AT _____ HRS

NB: HOURS ARE RELATIVE TO EARTHQUAKE ORIGIN TIME

5) SAFE DEPTH FOR CURRENT THRESHOLD OF 3 KNOTS _____ M

6) NOTE DURATION OF CURRENTS OVER THRESHOLD OF 3 KNOTS _____ HRS

IX) CURRENT ENVIRONMENTAL CONDITIONS

TIDE LEVEL AT ARRIVAL WILL BE: _____

TIDES IN FIRST 12 HOURS AFTER ARRIVAL WILL BE: _____

WIND/SWELL CONDITIONS _____

LONG WAVE ACTIVITY? _____

X) NOTES

Figure 6.8 Worksheet pages that should be printed and written on during an event response.

6.3 Playbooks for Historical Event Scenarios

In addition to the hypothetical scenarios modelled in this study, we also modelled the effects of five large-magnitude tsunami events known to have occurred in historical times. These include the 1700 Cascadia earthquake, the 1868 Arica, 1877 Iquique and 1960 Valdivia earthquakes in South America and the 2011 Tohoku Japan event. For each of these events we have produced a demonstration playbook sheet that can be used for reference. These were done to provide some degree of ground truthing for the overall products. An example of one of these sheets is presented in Figure 6.9 below.

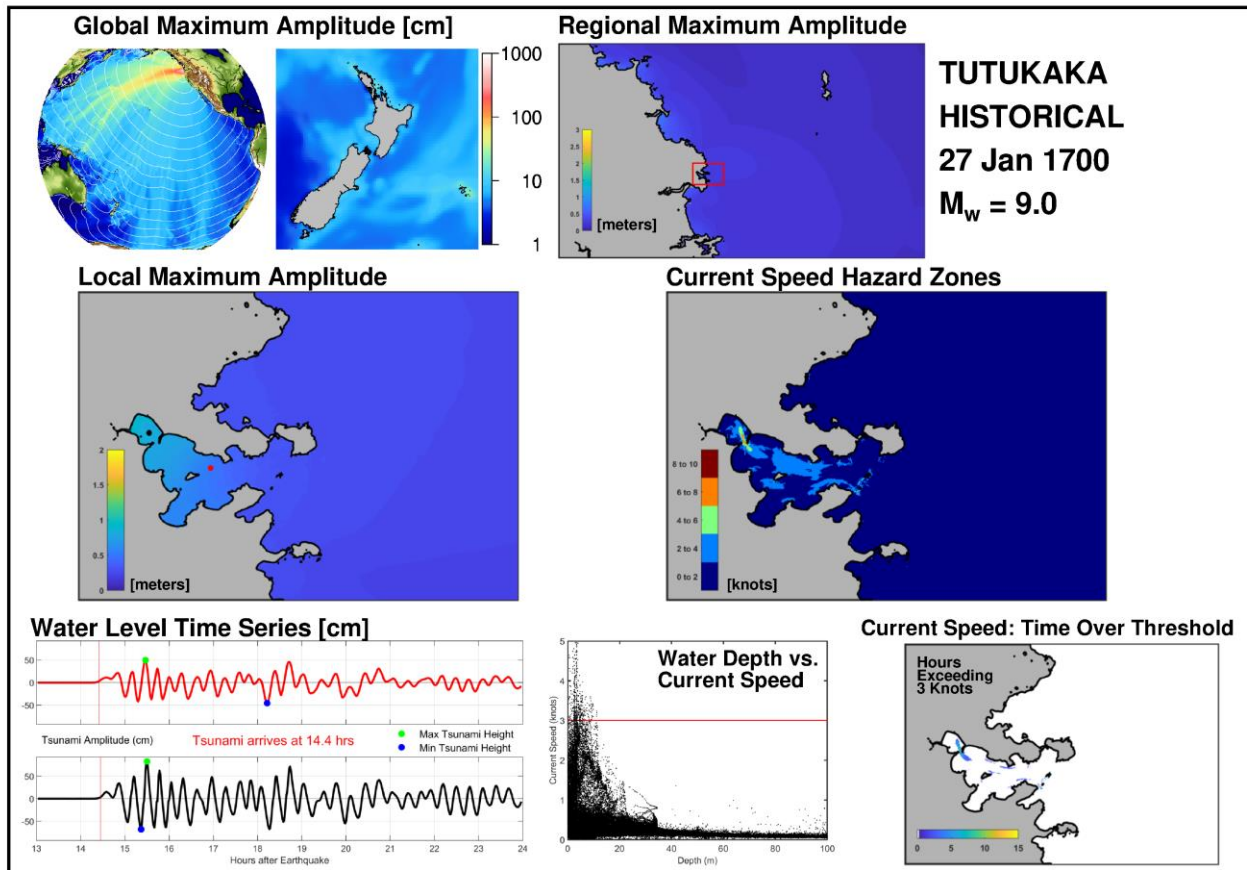


Figure 6.9 Sample playbook sheet for the AD 1700 Cascadia Subduction Zone tsunami affecting Tutukaka.

7 CONCLUSIONS

This report summarizes the development of a series of tsunami response playbooks for seven sites in the Northland region of New Zealand: Doves Bay, Marsden Point, Opuā, Tutukaka, Waitangi, Whangaroa Harbour and the entrance to Whangaroa Harbour. The playbooks contain detailed hydrodynamic modelling results including maximum tsunami water levels, maximum tsunami current speeds, tsunami current speed durations and an assessment of safe water depths for vessel evacuation. Tsunami scenarios from three large magnitude earthquakes (M_w 8.7, 9.0 and 9.3) were modelled for 72 source locations running counterclockwise around the Pacific rim from Southern Chile to the Southwest Pacific. Additionally, hindcast threat assessments were prepared for the seven sites based on five historical large magnitude earthquake and tsunami events including the 1700 AD event from the Cascadia Subduction Zone, the 1868, 1877 and 1960 events in South America and the 2011 event from Tohoku, Japan.

The outputs from this project are designed for use by Civil Defence and Emergency Management personnel and maritime officers of the Northland Regional Council enabling them to respond appropriately and in a timely manner to a particular tsunami event. Users can get to the pertinent information by navigating through three decision points related to the location and magnitude of the tsunami source. The opening pages of each playbook contain a two-page worksheet that should be printed and used during the event for recording important details relevant to the tsunami event underway. It is hoped that the results of this study will serve as a template or blueprint for the continued development of port and marina-specific tsunami response plans throughout New Zealand.

Future work should also focus on assessing the effects and developing playbooks for smaller local and/or regional events for which there would be sufficient time to implement such mitigation strategies. These efforts should focus on the most vulnerable sites such as Tutukaka responding to events on the TK Trench between East Cape and Tonga.

8 REFERENCES

- Amanda R. Admire, A., Dengler, L., Crawford, G., Uslu, B., Borrero, J.C., Greer, S. and Wilson, R. (2014) Observed and Modeled Currents from the Tohoku-oki, Japan and other Recent Tsunamis in Northern California, *Pure and Applied Geophysics*, 10.1007/s00024-014-0797-8.
- Arnold, J., Carter, J., Dumas, and Gillebrand, P. (2009) Northland Regional Council Tsunami Modelling Study 3 NIWA Client Report: CHC2009-042 June 2009
- Arnold, J., Gillebrand, P. and Sykes, J. (2011) Numerical modelling of tsunami inundation for Whangarei Harbour and environs NIWA Client Report: CHC2010-133 April 2011.
- Ayca, A. and Lynett, P. (2016) "Effect of Tides and Source Location on Nearshore Tsunami-Induced Currents." *Journal of Geophysical Research: Oceans*, doi: 10.1002/2016JC012435
- Beetham, R. D., McSaveney, M., Dellow, G., N., Rosenberg, M., Johnston, D. & Smith, W., 2004. A review of natural hazards information for Northland Region, Institute of Geological & Nuclear Sciences science report 2004/06 25 p.
- Borrero, J., Bell, R., Csato, C., DeLange, W., Greer, D., Goring, D., Pickett, V. and Power, W. (2012). Observations, Effects and Real Time Assessment of the March 11, 2011 Tohoku-oki Tsunami in New Zealand, *Pure and Applied Geophys.*, 170, 1229-1248, DOI 10.1007/s00024-012-0492-6
- Borrero, J.C. and Greer, S.D. (2012) Comparison of the 2010 Chile and 2010 Japan tsunamis in the Far-field, *Pure and Applied Geophysics*, 170, 1249-1274, DOI 10.1007/s00024-012-0559-4.
- Borrero, J.C., Goring, D.G., Greer, S.D., Power, W.L. and Barberopoulou, A. (2013) Decision Making Tools for the Real-Time Assessment of Far-Field Tsunami Hazards in New Zealand Ports and Harbours Part 1: Background Information and Preliminary Analysis. Prepared for New Zealand Ministry of Business Innovation and Employment, December 20, 2013.
- Borrero, J.C., Goring, D.G., Greer, S.D. and Power, W.L. (2014) Tsunami Hazards in New Zealand Ports, *Pure and Applied Geophysics*, 10.1007/s00024-014-0987-4
- Borrero, J.C., LeVeque, R.J., S. Dougal Greer, Sam O'Neill and Brisa N. Davis (2015a) Observations and Modelling of Tsunami Currents at the Port of Tauranga, New Zealand, *Proceedings of Coasts and Ports Conference*, Auckland, New Zealand, September, 2015.
- Borrero, J.C., Lynett, P.J. and Kalligeris, N. (2015b) Tsunami Currents in Ports, *Philosophical Transactions of the Royal Society A* , 373: 20140372. <http://dx.doi.org/10.1098/rsta.2014.0372>
- Borrero, J. (2017) Assessment of Tsunami Induced Currents in Indian Ocean Ports, *Proceedings of Coasts and Ports Conference*, Cairns, Australia, June, 2017
- Chagué-Goff, C. and Goff, J. (2006) Tsunami hazard assessment baseline for the Northland region, NIWA Client Report: CHC2006-069 June 2006
- De Lange, W.P. and Healy, T.R. (1986). New Zealand tsunamis 1840–1982. *New Zealand Journal of Geology and Geophysics*, 29(1), 115–134. doi:10.1080/00288306.1986.10427527
- Downes, G., A. Barberopoulou, U. Cochran, K. Clark, and F. Scheele (2017), The New Zealand Tsunami Database: Historical and Modern Records. *Seismological Research Letters*, 88 (2), 342-353, doi: 10.1785/0220160135.

- Fritz, H., Petroff, C., Catalán, P., Cienfuegos, R., Winckler, P., Kalligeris, N., Weiss, R., Barrientos, S., Meneses, G., Valderas-Bermejo, C., Ebeling, C., Papadopoulos, A., Contreras, M., Almar, R., Dominguez, J., and Synolakis, C. (2011a), Field survey of the 27 February 2010 Chile tsunami, *Pure Appl. Geophys.*, 168, 1989-2010.
- GeoNet (2017), M 7.1 East Cape Fri, Sep 2 2016 <http://www.geonet.org.nz/earthquake/2016p661332> Accessed June 22, 2017.
- Gillebrand, P., Lane, E., Arnold, J., Carter, J., Dumas, J. Enright, M. and Goff, J. and Roulston, H. (2008) Northland Regional Council Tsunami Modelling Study 2 NIWA Client Report: CHC2008-115 August 2008
- Goff, J. Walters, R. and Callaghan, F. (2006) Tsunami source study, NIWA Client Report CHC2006-082, August 2006.
- Goff, J., Pearce, S., Nichol, S. L., Chagué-Goff, C., Horrocks, M., & Strotz, L. (2010a). Multi-proxy records of regionally-sourced tsunamis, New Zealand. *Geomorphology*, 118(3-4), 369–382. doi:10.1016/j.geomorph.2010.02.005
- Goff, J., Nichol, S., Chagué-Goff, C., Horrocks, M., McFadgen, B., & Cisternas, M. (2010b). Predecessor to New Zealand's largest historic trans-South Pacific tsunami of 1868AD. *Marine Geology*, 275(1-4), 155–165. doi:10.1016/j.margeo.2010.05.006
- Kalligeris, N., Montoya, L., Ayca, A., and Lynett, P. (2017) "An Approach for Estimating the Largest Expected Tsunami from Far Field Subduction Zone Earthquakes." *Natural Hazards*, v. 89(1), pp. 233-253.
- Kalligeris, N., V. Skanavis, S. Tavakkol, A. Ayca, H. E. Safty, P. Lynett, and C. Synolakis (2016) "Lagrangian flow measurements and observations of the 2015 Chilean tsunami in Ventura, CA." *Geophysical Research Letters*, 43, doi: 10.1002/2016GL068796.
- Keen, A., Lynett, P., Eskijan, M., Ayca, A., and Wilson, R. (2017) "A Monte Carlo Based Approach to Estimate Fragility Curves of Floating Docks for Small Craft Marinas." *Journal of Waterway, Port, Coastal, and Ocean Engineering (ASCE)*, doi: 10.1061/(ASCE)WW.1943-5460.0000385
- Lane, E., Walters, R. Arnold, J. and Roulston, H. (2007) Northland Regional Council Tsunami Modelling Study 1 NIWA Client Report: CHC2007-109 September 2007
- Lynett, P., Borrero, J., Weiss, R., Son, S., Greer, D., Renteria, W. (2012) Observations and Modeling of Tsunami-Induced Currents in Ports and Harbors, *Earth and Planetary Science Letters*, 327-328 (68-74).
- Lynett, P.J., Borrero, J.C., Son, S., Wilson, R.W. and Miller, K. (2014) Assessment of the tsunami-induced current hazard, *Geophysical Research Letters*, DOI: 10.1002/2013GL058680
- New Zealand Palaeotsunami Database (2017). <https://ptdb.niwa.co.nz>, Accessed October 2018.
- Okal, E.A., H.M. Fritz, R. Raveloson, G. Joelson, P. Pancoskova, and G. Rambolamanana, (2006a) Madagascar field survey after the December 2004 Indian Ocean tsunami, *Earthquake Spectra*, 22, S263-S283.
- Okal, E.A., H.M. Fritz, P.E. Raad, C.E. Synolakis, Y. Al-Shijbi, and M. Al-Saifi, (2006b) Oman field survey after the December 2004 Indian Ocean tsunami, *Earthquake Spectra*, 22, S203-S218.
- Okal, E.A., A. Sladen, and E.A.-S. Okal, Rodrigues, (2006c) Mauritius and Réunion Islands, field survey after the December 2004 Indian Ocean tsunami, *Earthquake Spectra*, 22, S241-S261.

- Percival, D, Denbo, D, Eble, M, Gica, E, Mofjeld, H, Spillane, M, Tang, L, and Titov, V (2010). Extraction of tsunami source coefficients via inversion of DART buoy data, *Nat. Haz.* doi:10.1007/s11069-010-9688-1.
- Popovich, B (2015) Effects of Tsunami Loading on New Zealand Wharf Structures, University of Auckland Ph.D. Thesis
- Power, W and Gale, N. (2010) Tsunami Forecasting and Monitoring in New Zealand Pure and Applied Geophysics, DOI 10.1007/s00024-010-0223-9.
- Power, W. Downes, G. and Stirling, M. (2007) Estimation of Tsunami Hazard in New Zealand due to South American Earthquakes, *Pure and Applied Geophysics*, 164 (2007) 547-564 DOI 10.1007/s00024-006-0166-3.
- Power, W. L. (2013). Review of Tsunami Hazard in New Zealand (2013 Update) GNS Science Consultancy Report No. 2013/131, 238 pages.
- Power, W. L. (2014). Tsunami hazard curves and deaggregation plots for 20km coastal sections, derived from the 2013 National Tsunami Hazard Model GNS Science Consultancy Report No. 2013/59, 558 pages.
- Power, W., Borrero, J., Greer, D. and Goring, D. (2015) Developing robust tsunami forecasts for Ports and Harbours, Proceedings of the Australasian Coasts & Ports Conference 2015, 15 - 18 September 2015, Auckland, New Zealand. Available on-line.
- Shokin, *et al.*, 1987, Calculations of tsunami travel time charts in the Pacific Ocean, *Science of Tsunami Hazards*, vol. 5, p. 85-113.
- Todd, E. K., and T. Lay (2013), The 2011 Northern Kermadec earthquake doublet and subduction zone faulting interactions, *J. Geophys. Res.*, 118, doi:10.1029/2012JB009711
- Titov, V. V., & González, Frank, I. (1997). *Implementation and testing of the Method of Splitting Tsunami (MOST) model* (No. ERL PMEL-112) (p. 14). Retrieved from <http://www.pmel.noaa.gov/pubs/PDF/tito1927/tito1927.pdf>
- Titov, V. V., Moore, C. W., Greenslade, D. J. M., Pattiaratchi, C., Badal, R., Synolakis, C. E., & Kânoğlu, U. (2011). A New Tool for Inundation Modeling: Community Modeling Interface for Tsunamis (ComMIT). *Pure and Applied Geophysics*, 168(11), 2121–2131. doi:10.1007/s00024-011-0292-4
- Titov, V.V., and C.E. Synolakis (1995): Modeling of breaking and nonbreaking long wave evolution and runup using VTCS-2. *J. Waterways, Ports, Coastal and Ocean Engineering*, 121(6), 308–316.
- USGS (2016) M 7.0 - 175km NE of Gisborne, New Zealand <https://earthquake.usgs.gov/earthquakes/eventpage/us10006jb>, accessed on June 22, 2017.
- Wei, Y., Chamberlin, C., Titov, V. V., Tang, L., & Bernard, E. N. (2012). Modeling of the 2011 Japan Tsunami: Lessons for Near-Field Forecast. *Pure and Applied Geophysics*, 170(6–8), 1309–1331. <http://doi.org/10.1007/s00024-012-0519-z>
- Wei, Y, Newman, A, Hayes, G, Titov, V, Tang, L (2014). Tsunami Forecast by Joint Inversion of Real-Time Tsunami Waveforms and Seismic or GPS Data: Application to the Tohoku 2011 Tsunami. *Pure Appl. Geophys.* doi:10.1007/s00024-014-0777-z
- Wilson, R., Admire, A., Borrero, J., Dengler, L., Legg, M., Lynett, P., McCrink, T., Miller, K., Ritchie, A., Sterling, K., and Whitmore, P. (2012) Observations and Impacts from the 2010 Chilean and 2011 Japanese Tsunamis in California (USA), *Pure and Applied Geophysics*, DOI 10.1007/s00024-012-0527-z.

- Wilson, R. and Miller, K. (2012) Improving Tsunami Hazard Mitigation and Preparedness Using Real-Time and Post-Tsunami Field Data (abstract) American Geophysical Union, Fall Meeting 2012, abstract id. NH31C-1614.
- Wilson, R., Lynett, P., Eskijian, M., Miller, K., Laduke, Y., Curtis, E., Hornick, M., Keen, A. and Ayca, A. (2017) Tsunami Hazard Analysis and Products for Harbors in California (abstract) GSA Annual Meeting in Seattle, Washington, USA – 2017.